



UNIVERSIDAD DE INVESTIGACIÓN DE TECNOLOGÍA EXPERIMENTAL YACHAY

Escuela de Ciencias Químicas e Ingeniería

Integrated Study of Formation and Dissociation of THF Hydrates at Atmospheric Pressure

Trabajo de integración curricular presentado como requisito para la
obtención del título de Ingeniera en Polímeros

Autor/a:

Karen Estefanía Albán Jácome

Tutor/a:

PhD. Marvin Ricaurte

Urcuquí, Junio 2023

Autoría

Yo, **KAREN ESTEFANÍA ALBÁN JÁCOME**, con cédula de identidad 1717581001, declaro que las ideas, juicios, valoraciones, interpretaciones, consultas bibliográficas, definiciones y conceptualizaciones expuestas en el presente trabajo; así cómo, los procedimientos y herramientas utilizadas en la investigación, son de absoluta responsabilidad de el/la autor/a del trabajo de integración curricular. Así mismo, me acojo a los reglamentos internos de la Universidad de Investigación de Tecnología Experimental Yachay.

Urcuquí, Junio 2023.

Karen Estefanía Albán Jácome

CI: 1717581001

Autorización de publicación

Yo, **KAREN ESTEFANÍA ALBÁN JÁCOME**, con cédula de identidad 1717581001, cedo a la Universidad de Investigación de Tecnología Experimental Yachay, los derechos de publicación de la presente obra, sin que deba haber un reconocimiento económico por este concepto. Declaro además que el texto del presente trabajo de titulación no podrá ser cedido a ninguna empresa editorial para su publicación u otros fines, sin contar previamente con la autorización escrita de la Universidad.

Asimismo, autorizo a la Universidad que realice la digitalización y publicación de este trabajo de integración curricular en el repositorio virtual, de conformidad a lo dispuesto en el Art. 144 de la Ley Orgánica de Educación

Urcuquí, Junio 2023.

Karen Estefanía Albán Jácome

CI: 1717581001

Dedication

This work is dedicated to my wonderful and beloved family. To my dear mother Paulina whom I love with all my heart, who never stopped believing in me or in my dreams, who supported me in every step I took throughout my career and throughout my life, and never let me give up. To my sisters Catherine and Ariadna whom I adore infinitely, who with their joy and support always bring a smile to my face and motivate me to keep going against everything. To my grandmother Marlene, who with her support and love never stopped watching over my studies and well-being. To my uncle Christian, who always motivates me to want to go far, and supports me in each of my steps.

I also dedicate this thesis to my second family, to those amazing friends and colleagues who have accompanied and helped me throughout these years, especially Danny P., Melany A., Carlos A., Maithé R., Samantha Q., Erika M., Manuel M., Jimmy J. and Alexander S. I will always carry you in my heart.

Finally, I dedicate this work to my advisor Marvin Ricaurte, who has been able to guide me in my academic training, in addition to always providing me with the best possible advice throughout this thesis. Thank you for being not only my mentor, but also a great colleague and friend.

Karen Estefanía Albán Jácome

Acknowledgment

I want to deeply thank my family for always being by my side and for always supporting me in all my decisions. They are my pillar and my greatest treasure, I will always be grateful for motivating me to be a better person and professional every day.

I want to thank all the friends I made at Yachay Tech University for giving me the best moments and experiences I could have in my college life. Without you, the race would not have been so fun and motivating. I also want thank my beautiful roommies Melany and Kika, who never ever let me down and made living on campus very friendly and fun. I couldn't have wished for better housemates.

I am infinitely grateful to every professor I have met during my academic training, especially my advisor Marvin Ricaurte, for all his teachings, words of encouragement, for motivating me to never give up, and for helping me to grow day by day.

Finally, I thank Yachay Tech University and the School of Chemical Sciences and Engineering, for opening their doors to receive the best possible academic training, in order to become an excellent professional.

Karen Estefanía Albán Jácome

Resumen

Los hidratos son sólidos cristalinos formados a partir de agua con pequeñas moléculas en su estructura. Según la molécula encapsulada en su interior, los hidratos pueden clasificarse como hidratos líquidos o gaseosos. Actualmente, los hidratos de gas son una amenaza significativa para la industria del petróleo y el gas, por lo que su estudio es vital para minimizar su amenaza en estas áreas. Por ello, es necesario seleccionar correctamente un mecanismo de control de hidratos. Entre los mecanismos existentes se encuentra el uso de compuestos denominados "inhibidores", que controlan la tasa de formación de hidratos o modifican las condiciones termodinámicas de estabilidad de los mismos. Este trabajo se centra en el estudio del efecto inhibidor de varios inhibidores termodinámicos sobre la formación de hidratos de THF. El THF es un éter cíclico que forma hidratos líquidos a presión atmosférica. El estudio también incluye una propuesta alternativa de etanol artesanal para evaluar si es factible su uso como sustituto, tanto en eficacia como en conveniencia económica. Considerando la vocación agrícola del Ecuador y el uso de la química verde para valorizar y aprovechar desechos agroindustriales o fuentes naturales no comestibles, generando aditivos químicos para obtener inhibidores de hidratos. Como esto promueve el concepto de economía circular en el país, se estudia la producción de etanol artesanal a partir de la caña de azúcar como alternativa al uso de etanol industrial en el control de hidratos en industrias hidrocarburíferas. A partir del análisis de la temperatura de disociación de los hidratos, de diversos factores de pérdida y recuperación, y de varios estudios económicos de los diferentes precios de los inhibidores en el mercado, se determina finalmente cuál de todos los inhibidores propuestos es el más idóneo para utilizar como inhibidor de hidratos.

Palabras Clave: control de hidratos, hidratos de THF, inhibidores termodinámicos, alcohol, etanol

Abstract

Hydrates are crystalline solids formed from water with small molecules in their structure. Depending on the molecule encapsulated inside, hydrates can be classified as liquid hydrates or gas hydrates. Currently, gas hydrates represent a significant threat to the oil and gas industry, so their study is vital to minimize their threat in these areas. Therefore, it is necessary to select a hydrate control mechanism correctly. Among the various existing mechanisms is the use of compounds called "inhibitors", which control the hydrate formation rate or modify the thermodynamic conditions for hydrate stability. This work focuses on studying the inhibitory effect of several thermodynamic inhibitors on the formation of THF hydrates. The THF is a cyclic ether that forms liquid hydrates at atmospheric pressure. The study also includes an alternative proposal of artisanal ethanol to evaluate whether its use is feasible as a substitute, both in effectiveness and economic convenience. Considering Ecuador's agricultural vocation and the use of green chemistry to valorize and take advantage of agro-industrial wastes or inedible natural sources, generating chemical additives to obtain hydrate inhibitors. As this promotes the concept of circular economy in the country, the production of artisanal ethanol from sugar cane is studied as an alternative to the use of industrial ethanol in hydrate control in hydrocarbon industries. From hydrate dissociation temperature analysis, various loss and recovery factors, and several economic studies of the different inhibitor prices in the market, it is finally determined which of all the proposed inhibitors is the most ideal to use as a hydrate inhibitor.

Keywords: hydrate control, THF hydrates, thermodynamic inhibitors, alcohol, ethanol

Contents

Dedication	iii
Acknowledgment	iv
Resumen	v
Abstract	vi
Contents	vii
List of Tables	x
List of Figures	xi
1 Introduction	1
1.1 Problem statement	2
1.2 Objectives	4
1.2.1 General Objective	4
1.2.2 Specific Objectives	4
2 Theoretical Background	5
2.1 Natural gas	5
2.2 Hydrates: definition and classification	7
2.2.1 Type sI structure	9
2.2.2 Type sII structure	10
2.3 Hydrates formation prevention methods	11
2.3.1 Dehydration	12
2.3.2 Temperature control	13

2.3.3	Use of inhibitors	13
2.3.4	Hydrate control: which prevention method is the most optimal? . .	16
3	Methodology	17
3.1	Experimental setup	17
3.2	Proposed experimental methodology	18
3.2.1	Experimental tests preparation	18
3.2.2	Testing	18
4	Results and Discussion	21
4.1	Evaluation of the formation and dissociation of pure THF hydrates	21
4.2	Evaluation of the thermodynamic effects on THF hydrates dissociation of the proposed inhibitors	23
4.2.1	Ethanol	24
4.3	Ethanol production in Ecuador	25
4.3.1	Ethanol at 96%	25
4.4	Analysis and comparison of the inhibitory effects of each additive	27
4.5	Economic study: greater convenience among inhibitors.	30
4.5.1	Artisanal 96% ethanol: cost on the Ecuadorian market	31
5	Conclusions	32
	Bibliography	34
	Appendices	
A	Natural gas production in 2021	40
B	Hydrates formation and dissociation processes	41
B.1	Hydrate formation over time	42
B.2	Hydrate formation and dissociation varying P and T	43
C	Thermodynamic effects on THF hydrates dissociation of various inhibitors	45
C.1	Methanol	45
C.2	Butanol	45
C.3	Monoethylene Glycol (MEG)	46

D Hammerschmidt's equation: calculation of K constants associated with each inhibitor	48
D.1 Methanol	49
D.2 Ethanol	50
D.3 Butanol	50
D.4 Monoethylene glycol	51
D.5 96% Ethanol	51

List of Tables

2.1	Comparison of type sI, sII and sH structures.	9
2.2	Properties of some THL.	15
4.1	Dissociation temperatures of ice and THF hydrates as a function of 96% EtOH concentration.	26
4.2	Comparison of theoretical and experimental K_S values.	29
4.3	Comparison of theoretical and experimental K_H values.	29
C.1	Dissociation temperatures of ice and THF hydrates as a function of MeOH concentration.	45
C.2	Dissociation temperatures of ice and THF hydrates as a function of butanol concentration.	45
C.3	Dissociation temperatures of ice and THF hydrates as a function of MEG concentration.	46
D.1	ΔT_{dis} of ice and THF hydrates as a function of methanol concentration. . .	49
D.2	ΔT_{dis} of ice and THF hydrates as a function of ethanol concentration. . . .	50
D.3	ΔT_{dis} of ice and THF hydrates as a function of butanol concentration. . . .	50
D.4	ΔT_{dis} of ice and THF hydrates as a function of MEG concentration.	51
D.5	ΔT_{dis} of ice and THF hydrates as a function of 96% ethanol concentration.	51

List of Figures

1.1	Main risks associated with hydrates formation in natural gas industry. . . .	3
2.1	Natural gas constituents. (Ricaurte et. al, 2019)	6
2.2	Schematic representation of hydrates structures. (Rovetto, 2016)	8
2.3	Cages of Type sI hydrates. (Carroll, 2020)	9
2.4	Cages of Type II hydrates. (Carroll, 2020)	10
2.5	THF hydrates vs. Hydrocarbon hydrates structures. (Vlasic et al., 2019) .	11
2.6	Diagram of THF hydrates formation at different concentrations at 1 atm. (Wilson et al., 2005)	12
2.7	Effect of a kinetic inhibitor over hydrate formation in a pipeline.	14
2.8	Effect of a thermodynamic inhibitor over hydrate formation. (Olabisi et. al, 2015)	15
3.1	Adaptation of the PolyScience AD15R-40 circulating bath.	17
3.2	Schematic representation of the methodology developed in this study. . . .	20
4.1	Frozen solutions with different concentrations of THF.	22
4.2	THF hydrate dissociation process (visual monitoring)	22
4.3	Temperature curves comparison as a function of THF concentration for THF hydrates dissociation.	23
4.4	Temperature curve as a function of EtOH concentration for ice and THF hydrates dissociation.	24
4.5	Comparison of temperature curves as a function of EtOH (industrial and artisanal) concentration for ice and THF hydrates dissociation.	27

4.6	Thermodynamic inhibitory effects of various inhibitors on the ΔT_{dis} of ice and THF hydrates (19.2 wt%) curves.	28
A.1	Natural gas production in 2021 (units in bcm).	40
B.1	Hydrate nucleation process scheme. (Lv, Xiaofang et al., 2019)	42
B.2	Gas consumption vs. time diagram for hydrate formation. (Sloan and Koh, 2008)	42
B.3	Pressure vs. temperature diagram for methane hydrate formation. (Sloan and Koh, 2008)	44
C.1	Temperature curve as a function of MeOH concentration for ice and THF hydrates dissociation.	46
C.2	Temperature curve as a function of butanol concentration for ice and THF hydrates dissociation.	47
C.3	Temperature curve as a function of MEG concentration for ice and THF hydrates dissociation.	47
D.1	Excel spreadsheet for the estimation of K_S and K_H associated with methanol.	49
D.2	Excel spreadsheet for the estimation of K_S and K_H associated with ethanol.	50
D.3	Excel spreadsheet for the estimation of K_S and K_H associated with butanol.	51
D.4	Excel spreadsheet for the estimation of K_S and K_H associated with MEG.	52
D.5	Excel spreadsheet for the estimation of K_S and K_H associated with 96% ethanol.	52

Chapter 1

Introduction

Hydrates are crystalline compounds with an ice-like appearance formed from water molecules and other molecules smaller than them, which are encapsulated inside the hydrate structure. Depending on the type of encapsulated molecules, these crystalline solids can be classified in a general way as liquid hydrates or gas hydrates. [1] Although the great relevance of hydrates is fixed during the last decades up to the present due to the industrial era, these solids are hundreds of years old since their existence was first known.

These compounds were first discovered in 1778 when the scientist Joseph Priestley formed CO_2 hydrates in his laboratory. However, when defining the crystalline solids he obtained, he did not name them "hydrates". It was later, in 1811, when Sir Humphrey Davy reported the existence of chlorine hydrates, noticing the formation of "ice" above the usual freezing temperatures of an aqueous chlorine solution. However, even with the discovery of hydrates at that time, it was not until the 20th century that hydrates took on significant industrial relevance. In 1934 Hammerschmidt published the results of an inspection of the U.S. gas pipelines in a production plant, in which he reported the existence of frozen plugs formed inside the pipelines, hindering the correct transportation of gas. Initially, it was believed that these plugs were only made of ice because of their appearance. Still, when several samples were taken to a laboratory for analysis, it was determined that these solids were not purely made of ice but hydrates formed from the transported gas. [1, 2]

Since this discovery, studies on hydrate formation have been a very relevant topic, es-

pecially within the natural gas industry. These solids tend to agglomerate inside the pipelines at high pressures, causing blockages and putting production and personnel operating within the plant at significant risk. However, due to such operating conditions within the gas industry, hydrate formation studies within production plants can become difficult. Therefore, due to the difficulty of replicating systems that comply with the operating conditions of the natural gas industry, alternatives can be found that allow hydrate studies to be carried out under more manageable conditions. A good option for studying gas hydrate formation is to employ systems at atmospheric pressure, using tetrahydrofuran (THF) as the hydrate-forming model molecule. This organic compound has the particularity of forming the same type of crystalline structure as the hydrates that form inside natural gas pipelines, but at atmospheric pressure, making it more accessible to study the hydrate formation on a laboratory scale. [3]

1.1 Problem statement

Among the goals of the gas and oil industries is to mitigate the costs associated with operational and structural failures as much as possible, maintain optimal working security for personnel, and offer the best possible quality of their products. [4] Due to the operational and economic challenges of absolute and complete control of plant operations, several problems arise when processing, transporting, and storing the product. Figure 1.1 shows the main risks caused by hydrates formation within the natural gas industry. [4, 5]

- **Problems in flow assurance:** the formation of hydrates inside the pipelines causes plugging, obstructing the correct flow of gas through the pipelines, which could negatively affect the plant operation. Hydrates can also perforate pipelines if, instead of agglomerating, they form as projectiles traveling along with the gas flow at high pressures; perforating a pipeline causes the flow to leak.
- **Equipment damage:** as hydrate solids form inside the pipelines, they travel through the pipeline networks and can reach the different equipment used in the production lines, creating the possibility of costly or irreparable damage to the pipelines and equipment.

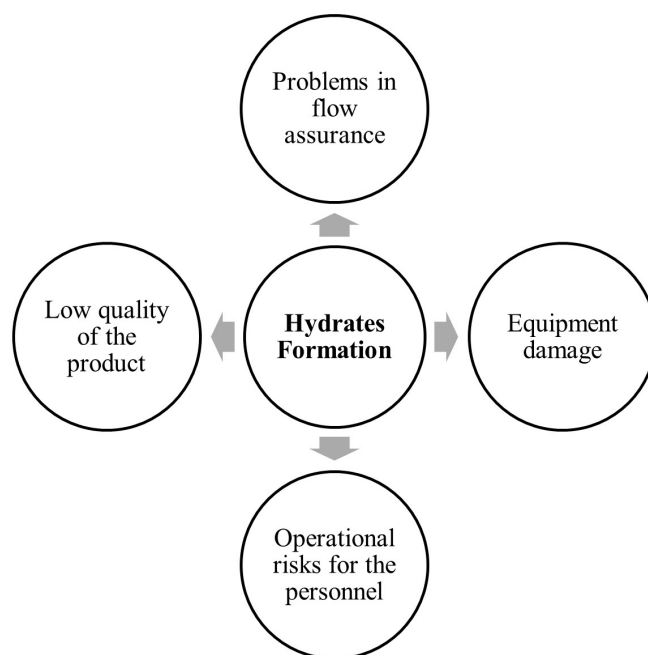


Figure 1.1: Main risks associated with hydrates formation in natural gas industry.

- **Operational risks for the personnel:** hydrates that form and travel in the natural gas flow can cause severe damage, such as perforation or blockage of the pipelines. When high pressures are handled in plant operation, toxic or flammable leaks or pipeline bursts may occur. Plant personnel are exposed to these hazards if hydrate formation is improperly controlled or prevented.
- **Low product quality:** hydrates not only permanently damage the plant equipment but can also alter its correct operation, decreasing the plant's performance efficiency and resulting in poor quality products downstream. This causes production delays and generates unnecessary and avoidable economic expenses.

It is crucial to carry out studies that analyze the formation and dissociation of hydrates to reduce as much as possible and even avoid the problems caused by them in pipelines and equipment. To work with a system at atmospheric pressure at a manageable laboratory scale, in the studies carried out to analyze the hydrate behavior, the THF can be used since it is similar to that of gas hydrate structure. Once the results of these studies have been reported, various inhibiting additives can be tested and proposed to help control the hydrate formation.

1.2 Objectives

1.2.1 General Objective

To comprehensively study the formation and dissociation of tetrahydrofuran hydrates at atmospheric pressure conditions.

1.2.2 Specific Objectives

- To develop and fine-tune of a methodology to study the behavior of THF hydrates at laboratory scale.
- To select various thermodynamic inhibitors for analysis of their effectiveness in hydrate control.
- To make an alternative proposal to use one of the selected industrial inhibitors.
- To conduct studies on the hydrate dissociation temperature under the effect of each of the inhibitors to select the most suitable ones.
- To complement the selection of the most convenient inhibitor, it also considers its economic convenience by studying its prices in the market.

Chapter 2

Theoretical Background

2.1 Natural gas

Natural gas is a gaseous fossil fuel that can be found in oil and natural gas fields located in subsurface rock reservoirs. Due to the locations where natural gas is extracted, it is sometimes associated with crude oil and is called "associated natural gas"; when extracted without the presence of crude oil, it is called "non-associated natural gas". It is considered one of the most widely fuels used worldwide due to its efficiency and clean burning. That is why the natural gas-producing industry has a large extension worldwide.

According to gas market data for 2021, production is expected to increase by 4.6% compared to 2020, mainly concentrated in North America and Europe, in countries such as the United States and Russia, with a production of 975 and 791 bcm (billion cubic meters) of natural gas respectively. In South America, Argentina, Brazil, and Colombia stand out as producers, with 41, 25, and 12 bcm, respectively. [6] A graphical representation of the data at the global level on a map can be found in Appendix A. [7]

Ecuador is also among the South American countries that produce natural gas on a smaller scale. In 2021, production in the Amistad gas field (operated by Petroecuador) was 28.8 million cubic feet per day, corresponding to approximately 300 million cubic meters of natural gas annually. [8]

Natural gas is formed of a mixture of various hydrocarbons such as methane, ethane, propane, etc., and some non-hydrocarbons like hydrogen sulfide, carbon dioxide, water, etc. [1, 9, 10] A compilation of all the constituents found in natural gas, as well as the proportions usually present in lean and rich gas, can be found in Figure 2.1

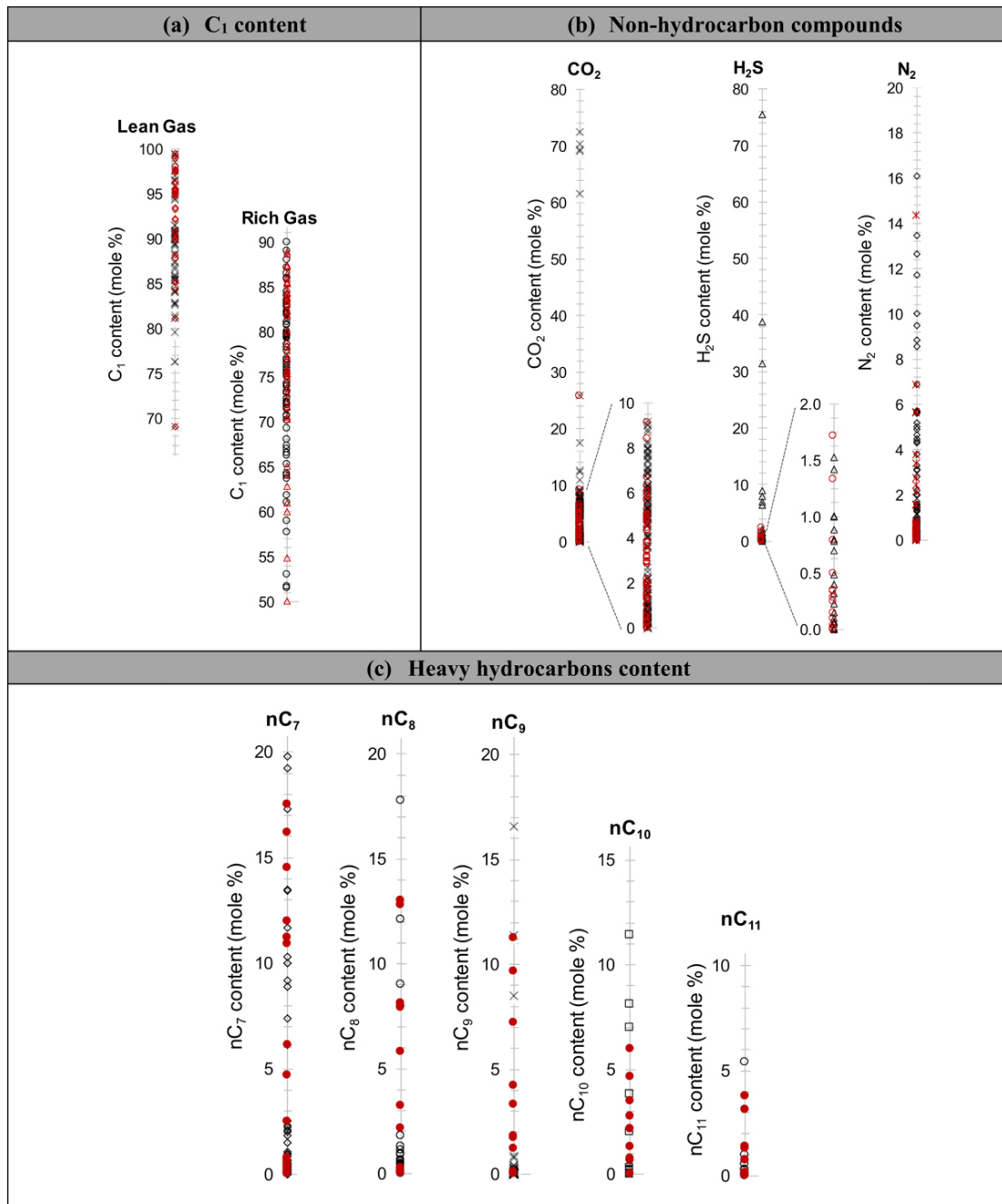


Figure 2.1: Natural gas constituents. (Ricaurte et. al, 2019)

Hydrocarbon components can be used as lubricants, as fuels (mainly used for power generation, in industries, commercially, in residences and transportation), and as feedstocks in industry (production of plastics, fibers, rubbers, solvents, explosives and various industrial chemicals). Non-hydrocarbon components do not usually have as much value or applications when talking about its presence in natural gas. [11]

However, many of these components of natural gas (both hydrocarbons and non-hydrocarbons) combine with water to form components known as "gas hydrates". As natural gas is expected to be extracted during subsurface extraction, non-depreciable amounts of water accompany it. This represents a significant problem in production, processing, and transportation since the operational conditions are favorable for forming hydrates inside the pipelines and equipment. [9]

2.2 Hydrates: definition and classification

Hydrates are crystalline solids with an ice-like appearance, consisting of water molecules and organic or inorganic compounds whose molecules are smaller than water. These solids have a particular crystalline structure since the water molecules form a network between them, which has cages where the smaller molecules are housed. In these arrangements, the water molecules are called "host molecules", while the molecules inside the cages are called "guest molecules". The guest molecules are also called "formers" and stabilize the crystal structure; they can be molecules of a gas or liquid compound. Three conditions are necessary for them to be formed, which are:

- Suitable pressure and temperature conditions. Usually, these are high pressures and low temperatures; however, there are liquid formers that can form hydrates at atmospheric pressures (e.g. tetrahydrofuran, dioxolane and cyclopentane).
- A former must always be present. Without these molecules occupying the available cages in the crystal structure, stability is not necessary for hydrate formation.
- Presence of water, but not in excessive quantities.

Processes related to hydrate formation and dissociation when these conditions are met can be found in Appendix B.

Once the three conditions necessary for hydrate formation are reached, hydrates can take on different types according to their crystalline structure. [1, 4, 5] There are 3 ways to classify them: structures type sI, sII and sH. Figure 2.2 shows a diagram of the classification of hydrates according to their structure. [12]

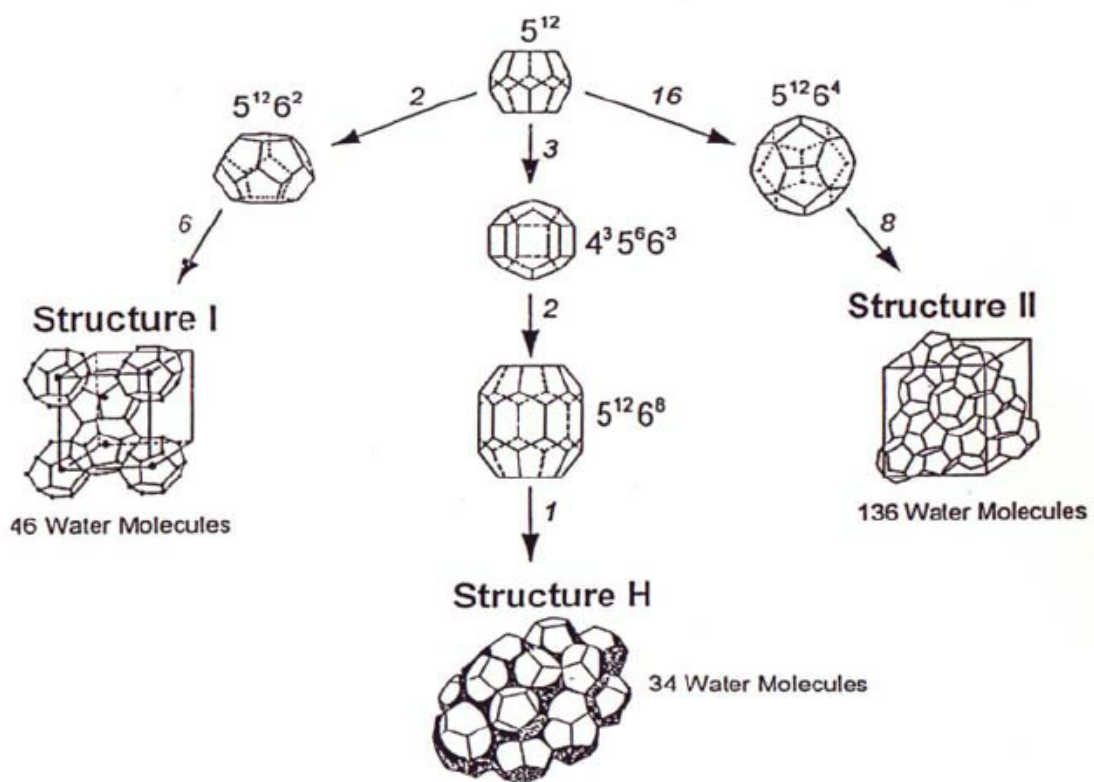


Figure 2.2: Schematic representation of hydrates structures. (Rovetto, 2016)

Type sI and sII are the most commonly formed (these structures belong to hydrates formed during oil and gas production and processing) and sH the most unusual. Each type of structure is composed of different cages where the formers are hosted, which have the shape of polyhedra. To identify each of these polyhedra, it is used the nomenclature $n_i^{m_i}$, where n_i represents the number of edges in the face "i", and m_i is the number of faces of the polyhedron. [13] Table 2.1 shows a comparative summary of type sI, sII, and sH structures.

Table 2.1: Comparison of type sI, sII and sH structures.

Structure type	sI		sII		sH		
Cavity type	Small	Large	Small	Large	Small	Medium	Large
Description	5^{12}	$5^{12}6^2$	5^{12}	$5^{12}6^4$	5^{12}	$4^35^66^3$	$5^{12}6^8$
Cages per unit cell	2	6	16	18	3	2	1
Water molecules	46		136		34		
Theoretical formula ¹	$X \cdot 5 \frac{3}{4}H_2O$		$X \cdot 5 \frac{2}{3}H_2O$		$5X \cdot Y \cdot 34H_2O$		

¹ Where X belongs to the hydrate former and Y is a Type sH former.

2.2.1 Type sI structure

Type sI structure is the simplest of the three types of hydrate structures. Its crystal network comprises two cages: dodecahedron (5^{12}) and tetrakaidecahedron ($5^{12}6^2$). Figure 2.3 shows a visual representation of cages present in type sI hydrate structure.

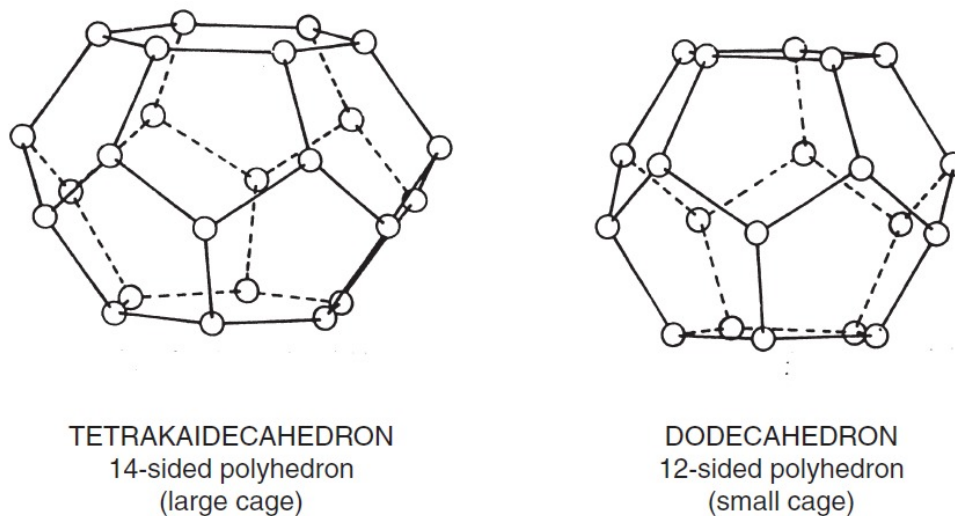


Figure 2.3: Cages of Type sI hydrates. (Carroll, 2020)

For each unit cell, 46 water molecules can be found, and their associated formula for the hydrate structure in case a guest molecule occupies all the cages, is $X \cdot 5 \frac{3}{4}H_2O$. The most common formers for this type of hydrate are methane, ethane, carbon dioxide, and hydrogen sulfide. [1, 4]

2.2.2 Type sII structure

Type sII structure is slightly more complicated than type sI structure. Its crystal network comprises two cages: dodecahedron dodecahedron (5^{12}) and hexakaidecahedron ($5^{12}6^4$). Figure 2.4 shows a visual representation of the cages in type sII hydrate structure.

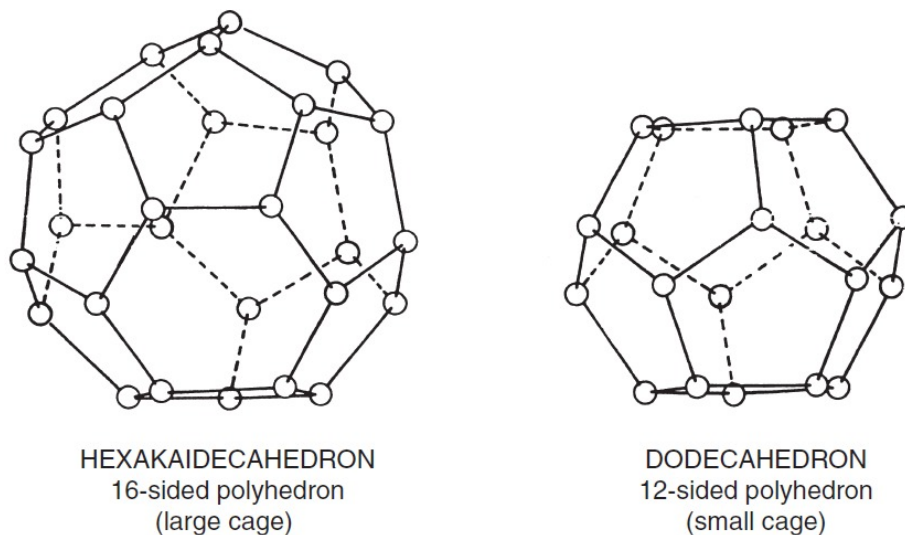


Figure 2.4: Cages of Type II hydrates. (Carroll, 2020)

For each unit cell, 136 water molecules can be found, and their associated formula for the hydrate structure in case a guest molecule occupies all the cages, is $X \cdot 5 \frac{2}{3} H_2O$. The most common formers for this type of hydrate are gas compounds, like nitrogen, propane, and iso-butane. Another compound capable of forming this type of hydrate and which does not belong to any component of natural gas is tetrahydrofuran.[1, 4]

THF hydrates

Tetrahydrofuran (THF) is a cyclic-ether compound whose molecular formula is $(CH_2)_4O$. Although this compound is often used mainly as a solvent or precursor in the synthesis of various polymers, [14] it is also a compound that can be used in studying hydrates. THF can form clathrates with a type sII hydrate structure, the same type of structure formed by natural gas hydrates.

However, the peculiarity of these hydrates is that, unlike natural gas hydrates, they do not form at high pressures; they form at atmospheric pressures and temperatures above

0°C. Figure 2.5 compares the structures formed by both THF hydrates and natural gas hydrates (hydrocarbons). It can be seen that both are almost identical, which makes it possible to propose THF hydrates as a model system for the study of hydrates at atmospheric pressure. [15, 16]

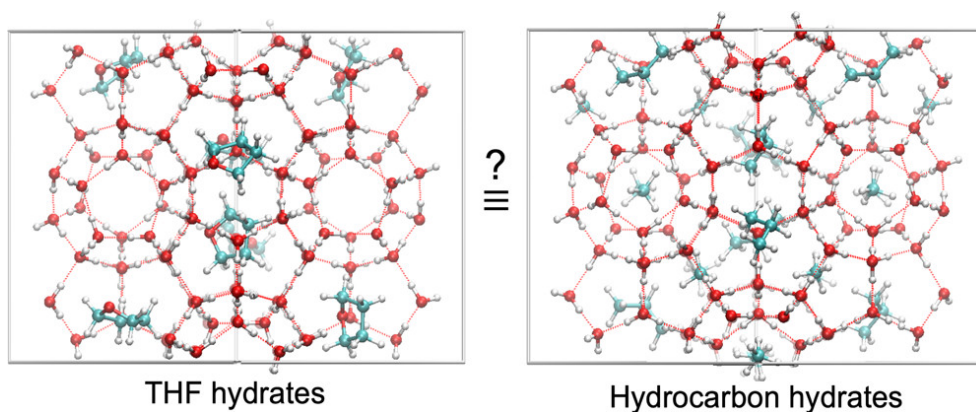


Figure 2.5: THF hydrates vs. Hydrocarbon hydrates structures. (Vlasic et al., 2019)

THF is capable of forming hydrates at different temperatures depending on the water/THF ratio of the hydrate-forming solution. This can be best visualized in Figure 2.6, where the different hydrate-forming temperatures of THF are presented when the mass ratio of THF to water varies. One point in particular (marked with a red cross), stands out from this diagram, which corresponds to the highest value of the melting point. This is 4.45 °C and it is reached when the THF concentration in the solution is 19.2 %w/w; at this point the hydrate is completely stoichiometric (17:1 mol ratio). [15]

2.3 Hydrates formation prevention methods

The hydrate formation of hydrates is a critical problem in the natural gas and oil industries since they could block the pipelines and cause severe damage to the production process, the machinery, and operating personnel. For this reason, there are some techniques for the inhibition of hydrate formation, [17] among which are:

- Remove the water present in the gas mixture through the dehydration process.
- Perform a temperature modification.
- Use of inhibitors.

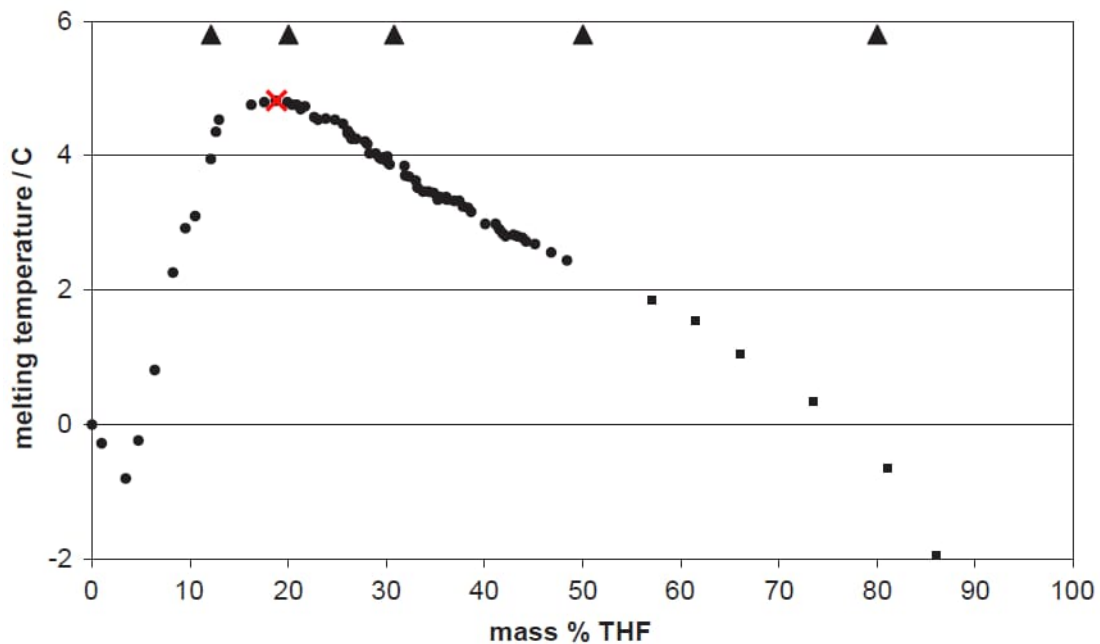


Figure 2.6: Diagram of THF hydrates formation at different concentrations at 1 atm. (Wilson et al., 2005)

2.3.1 Dehydration

This process removes the water present in a gaseous stream. Two main methods are used for this purpose: absorption using glycols and adsorption employing solid desiccants. [17]

Absorption process

Liquid desiccants (glycols) are used in this technique. Triethylene glycol (TEG) is generally used in a dehydration unit located at the natural gas plant. The TEG is circulated at high concentrations to achieve the highest possible water absorption and then recovered to remove the water from the system and reuse the glycol for further recirculation. [18]

Adsorption process

In this technique, solid desiccants are used within an adsorption bed. This process occurs when the water molecules in the gas stream come into contact with the solid surface of the desiccants and condense on it. A layer is formed that remains attached to the adsorption surface until later removed. The most commonly used desiccants are the following:

- Alumina

- Silica gel
- Molecular sieves

An essential characteristic of these solids is that they have a large effective surface area and can be regenerated for further use. [19]

2.3.2 Temperature control

This method is typically used in offshore systems. It consists of increasing the gas flow temperature so that it reaches a value above the equilibrium point of the hydrate in question. Thus, the optimal temperature condition for forming hydrates cannot be given. [5] This can be applied through: heated bundles, electrical heating, heating tents, mud/fluid circulation and external heat tracing.

2.3.3 Use of inhibitors

A kinetic or thermodynamic inhibition effect is achieved depending on the type of chemical applied. The use of chemicals such as polar solvents (for example, alcohols or glycols) or water-soluble polymers is employed. However, thermodynamic inhibitors are more widely used within the natural gas industry than kinetic ones.

Kinetic inhibitors

Kinetic hydrate inhibitors or KHIs have water-soluble polymer formulations with amphiphilic groups like amides and some hydrophobic groups with 3 to 6 carbon atoms. As can be seen in Figure 2.7, the way in which these inhibitors work is by reducing the speed of nucleation and growth of the hydrates for some time.

However, it is not guaranteed that hydrates will not appear since you are only delaying their formation. At some point, they will form. In addition, another reason why this type of chemical is not widely used is due to its high costs since it is one of the most

expensive oilfield production chemicals. [20]

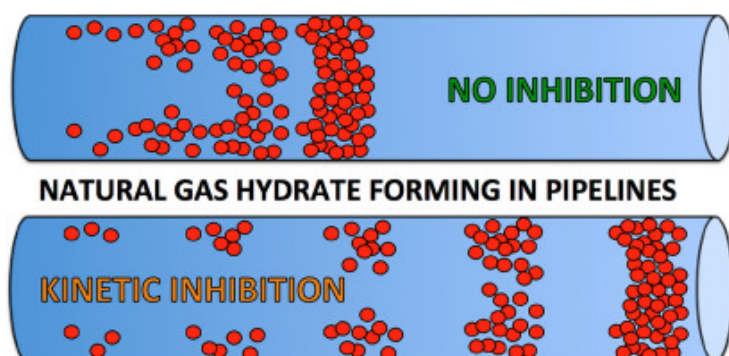


Figure 2.7: Effect of a kinetic inhibitor over hydrate formation in a pipeline.

Thermodynamic inhibitors

Thermodynamic hydrate inhibitors (THI) are generally compounds of alcohols, glycols or even ionic salts. The most commonly used THIs are the following: methanol, ethanol, monoethylene glycol and triethylene glycol. Other compounds belonging to the alcohol and glycol families are also used but to a lesser extent (e.g., propanol or diethylene glycol).

It is essential to mention that, as their name indicates, the THI only inhibits the formation of hydrates but does not entirely prevent their formation, as this could happen at some point. [1] However, how THI work is by causing the temperature and pressure conditions at which hydrates are usually formed to be affected. That is, the formation temperature will be lower, and the formation pressure will be higher. [21] This can be seen in Figure 2.8, where it can be observed that the original equilibrium curve of a hydrate, when a THI is added, shifts to the left, creating more range in the hydrate-free zone and consequently reducing the risk zone for the appearance of hydrates. [22]

To explain why these compounds can shift the hydrate equilibrium curve, Table 2.2 presents some properties of some THI. Each of these compounds has the presence of hydrogen bonds in its molecular composition. Therefore, when added to a natural gas stream with traces of water, they can interfere with and inhibit the hydrogen bonds of the water present. [1]

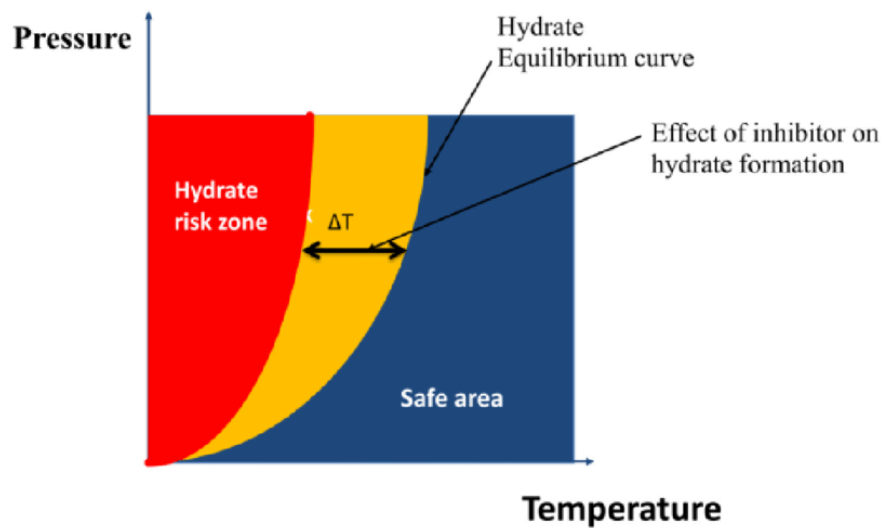


Figure 2.8: Effect of a thermodynamic inhibitor over hydrate formation. (Olabisi et. al, 2015)

Table 2.2: Properties of some THI.

	MeOH	EtOH	Propanol	EG	TEG
Empirical formula	CH_4O	C_2H_6O	C_3H_8O	$C_2H_6O_2$	$C_4H_{10}O_3$
Molar mass, g/mol	32.042	46.07	60.09	62.07	150.17
Boiling point, °C	64.7	78.4	97	198	288
Melting point, °C	-98	-112	-126	-13	-4.3
Density, kg/m^3	792	789	803	1116	1126

Hammerschmidt equation

One way of estimating the effect of an inhibitor on the hydrate formation temperature is the Hammerschmidt equation

$$\Delta T = \frac{K_H}{M} \left(\frac{W}{100 - W} \right)$$

where ΔT corresponds to the temperature depression (in °C), K_H is the Hammerschmidt constant associated with each inhibitor, M is the molar mass of the inhibitor used (in g/mol), and W is the weight percent concentration (wt%) of the inhibitor in the aqueous phase. [1] This equation is easy to apply and works well for various thermodynamic inhibitors (except for ionic solid-type inhibitors).

2.3.4 Hydrate control: which prevention method is the most optimal?

Several methods prevent hydrate formation, including dehydration, temperature control, and inhibitors. However, some of these methods involve the installation of extra equipment or complements beyond the the pre-established operational design of a natural gas production, treatment or transportation plant. Nevertheless, the threat posed by the presence of hydrates in the industry should not be overlooked, so the selection of the most appropriate hydrate control method is necessary. Therefore, it is proposed that the most convenient method of inhibiting hydrate formation would be the use of inhibitors.

A good proposal for the study of the effects of both thermodynamic or kinetic inhibitors is the use of a system that allows operating at atmospheric pressure conditions for better experimental management and data collection to conduct various tests to determine the effectiveness of this inhibitors. For this purpose, tetrahydrofuran (THF) was selected as the hydrate-forming compound because it forms the same type (sII) of hydrocarbon hydrates, in addition to having the particularity of being able to form hydrates at atmospheric pressure.

Chapter 3

Methodology

3.1 Experimental setup

A PolyScience circulation bath, model AD15R- 40-A11B, was adapted for the proposed study. It has a capacity of 15 liters and a digital monitor controller that allows controlling the temperature range of the bath, which goes from $-40\text{ }^{\circ}\text{C}$ to $200\text{ }^{\circ}\text{C}$.

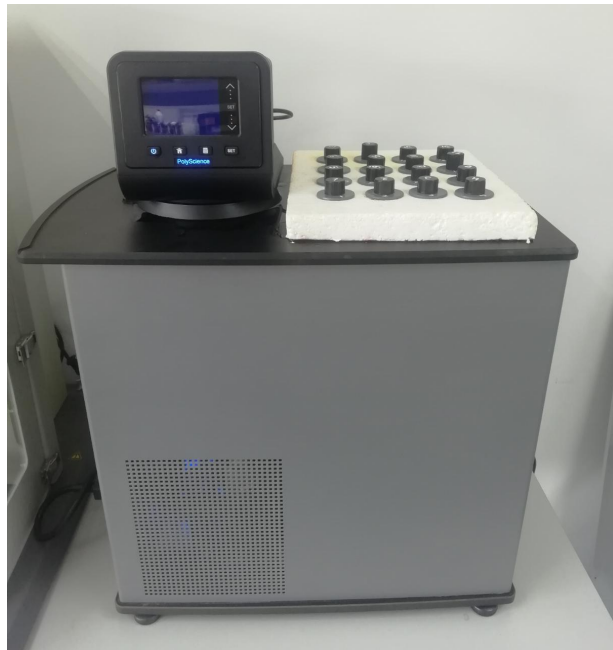


Figure 3.1: Adaptation of the PolyScience AD15R-40 circulating bath.

As in Figure 3.1, the equipment was adapted to assemble and perform the established tests. First, the tank was filled with a solution of polyethylene glycol and water in a 1:1 volume ratio as the fluid to cool the samples. Then, a polystyrene plate with 16 round cavities to

place the test tubes was attached to the space where the tank cover would be placed. To complement the adaptation, flat washers were placed on top of these cavities to prevent the test tubes from sinking into the tank.

3.2 Proposed experimental methodology

To perform the various experimental tests related to the formation and dissociation of THF hydrates, in addition to the subsequent tests with various thermodynamic inhibitors, it is proposed to prepare 16 different samples. These are placed in test tubes, with a content of 5 g each one, according to the type of experimental tests to be performed. These tubes are cooled to freezing in the PolyScience circulation bath tank, with the help of the previously adaptation.

3.2.1 Experimental tests preparation

THF hydrates samples

In order to test the proposed methodology for the study of THF hydrates, in addition to corroborate the results obtained by the same together with results from the literature, a sample of distilled water and 15 solutions of THF and distilled water were prepared at 5, 10, 19.2, 30, and 40 wt%. Each of the THF solutions was prepared in triplicate.

Inhibitors effect evaluation

For this experimental sets using alcohol or glycol type inhibitors, 8 solutions were prepared from solutions of 19.2 wt% THF and the selected inhibitor in proportions of 5, 10, 20, and 40 wt%. Eight solutions of the selected inhibitor and distilled water at 5, 10, 20, and 40 wt% were also prepared.

3.2.2 Testing

Each of the experimental sets was carried out as follows:

1. The solutions were prepared according to each set and placed in test tubes.

2. The test tubes were taken to the circulating bath to be placed in the adaptation that was made.
3. An initial temperature of $-30\text{ }^{\circ}\text{C}$ is placed in the circulation bath.
4. Once the samples were crystallized, monitoring was performed every day, twice a day (8 am and 4 pm). All test tubes were checked at each monitoring to see if any sample had dissociated; this is determined when the samples (which were initially frozen) return to a fully liquid state. In addition, for each monitoring, the bath temperature was also raised by 0.5 or $1\text{ }^{\circ}\text{C}$.

Figure 3.2 shows a schematic representation of the methodology developed in this study. It is divided into three sections: experimental setup assembling, evaluation of THF hydrates and evaluation of the inhibitory effect of the proposed inhibitors on THF hydrates.

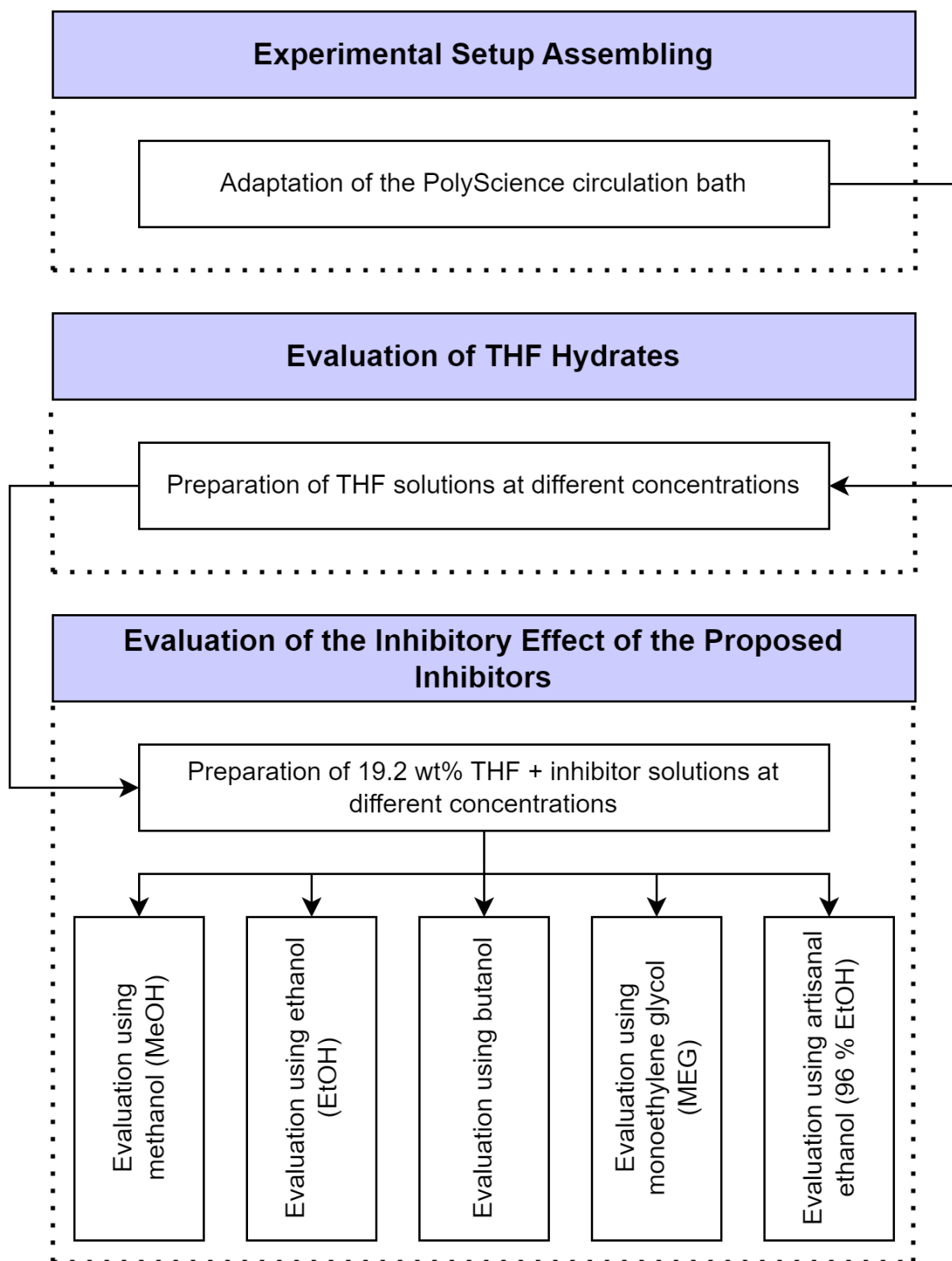


Figure 3.2: Schematic representation of the methodology developed in this study.

Chapter 4

Results and Discussion

4.1 Evaluation of the formation and dissociation of pure THF hydrates

In order to prove that the proposed methodology is efficient for the study of THF hydrates, as well as to be able to contrast the experimentally obtained results with results of Wilson et. al (2005), samples were prepared at different THF concentrations. Since the stoichiometric point of interest is at a THF concentration of 19.2 wt%, the study was limited to preparing THF solutions at 40 wt%. For visual observation of each of the samples prepared and taken to freezing, see Figure 4.1. Each solution at different concentrations was performed in triplicate.

For the determination of the dissociation of the hydrate samples, the test tubes were observed as the bath temperature was gradually increased. Dissociation process of a THF hydrate sample, from initial freezing to complete dissociation, can be seen in the Figure. 4.2

Once the data were collected, a comparison was made of the temperature curves obtained experimentally and the data obtained by Wilson et al. (2005), which is reflected in Figure 4.3. The points obtained experimentally and reflected in the curve show a trend very close to the theoretical curve. In addition, these are within the margin reflected by error bars, which completely validates the data obtained in this first experimental set, confirming that the proposed study methodology is adequate for subsequent experiments with inhibitors.

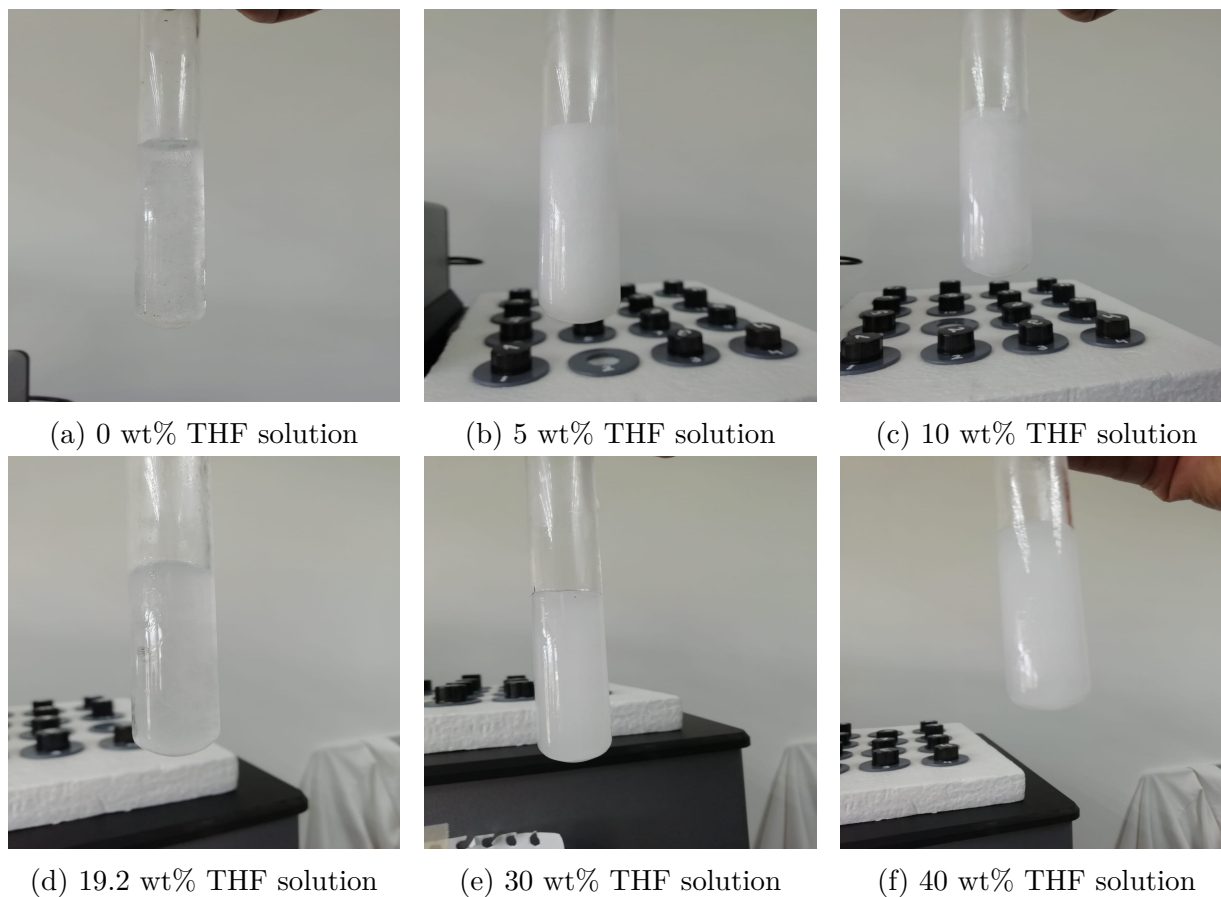


Figure 4.1: Frozen solutions with different concentrations of THF.

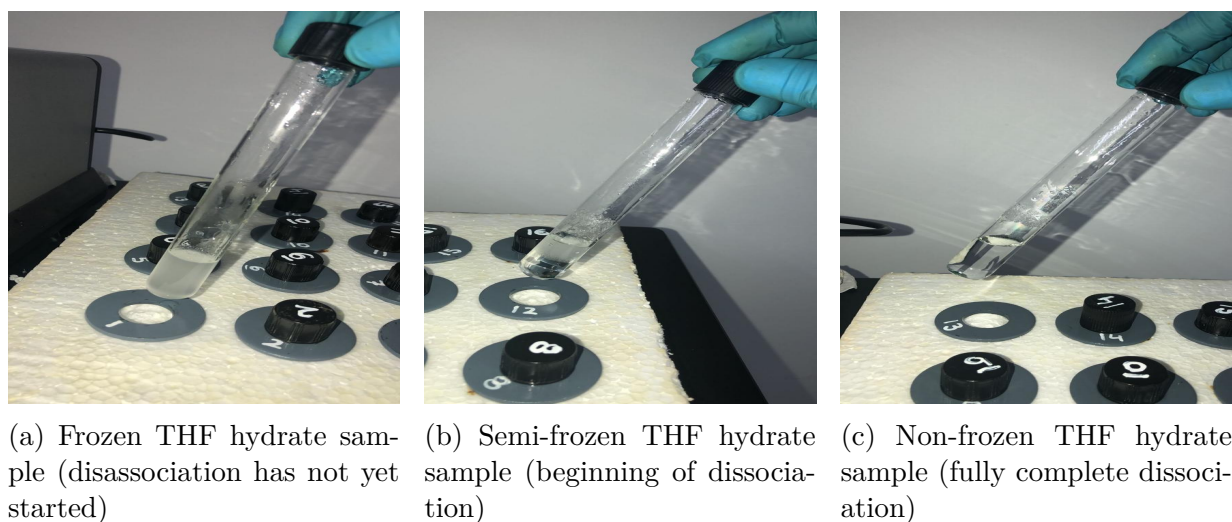


Figure 4.2: THF hydrate dissociation process (visual monitoring)

After experimental data validation, the stoichiometric point of interest, whose THF concentration is 19.2 wt% and dissociation temperature is 4.5 °C, is chosen for the tests with various thermodynamic inhibitors.

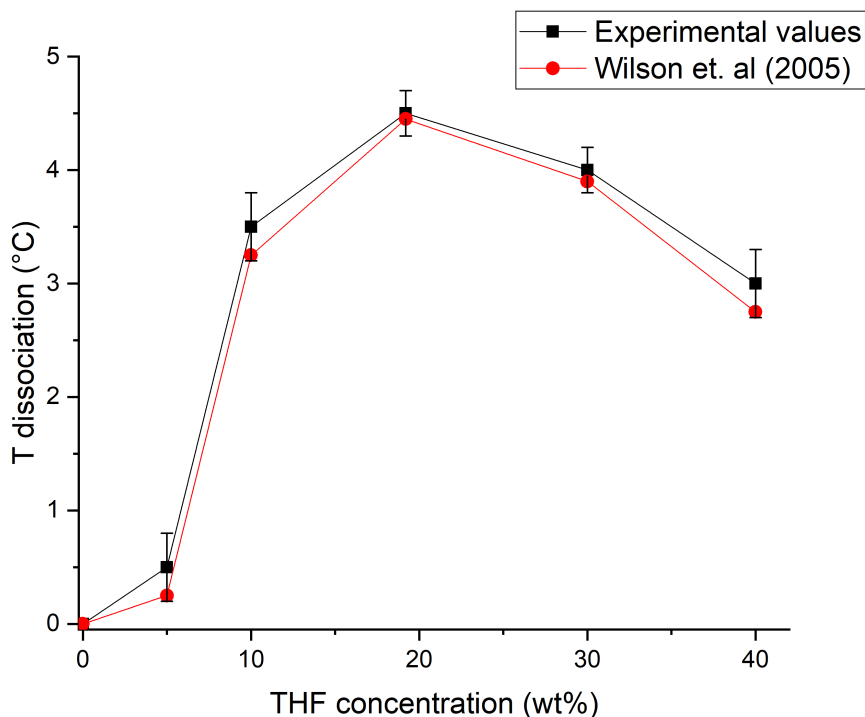


Figure 4.3: Temperature curves comparison as a function of THF concentration for THF hydrates dissociation.

4.2 Evaluation of the thermodynamic effects on THF hydrates dissociation of the proposed inhibitors

For the tests to be performed using each of the proposed inhibitors to study their effect on THF hydrates, these compounds were applied at different concentrations to solutions of 19.2 wt% THF (stoichiometric solution) and distilled water. The chosen concentrations of the inhibitors to be applied (methanol, both ethanols, butanol and MEG), were 5, 10, 20 and 40 wt%; all of these samples were prepared in duplicate. Samples with 40 wt% inhibitor concentration failed to reach freezing because the circulation bath failed to go below -15 °C.

Because several inhibitors with the same effect on THF hydrate dissociation (on a smaller or larger scale in each case) are used, it was decided to choose ethanol for a more detailed analysis. The experimental data obtained from the tests with the rest of the inhibitors that are not found in this section (dissociation temperatures of the samples and curves

generated from them) can be found in Appendix C.

4.2.1 Ethanol

One of the chosen compounds to be thoroughly evaluated, which also belongs to the alcohol family, is ethanol. This compound was chosen because two types of ethanol are used, which will enable a comparison of the inhibitory effect of both compounds. In addition, it allows a more in-depth analysis of ethanol as an inhibitor, since most studies usually focus on methanol or MEG instead of EtOH. As in the THF hydrate formation and dissociation study, this study is carried out based on the same type of methodology proposed, also taking into account the addition of the inhibitor in different concentrations.

The experimental results related to the tests with ice and hydrates are reflected in Figure 4.4. As additional validation of the data obtained, specifically for the ice curves, they were compared with studies previously performed in Cheremisinoff, Nicholas P (2003) [23], determining that using the proposed methodology our data are valid.

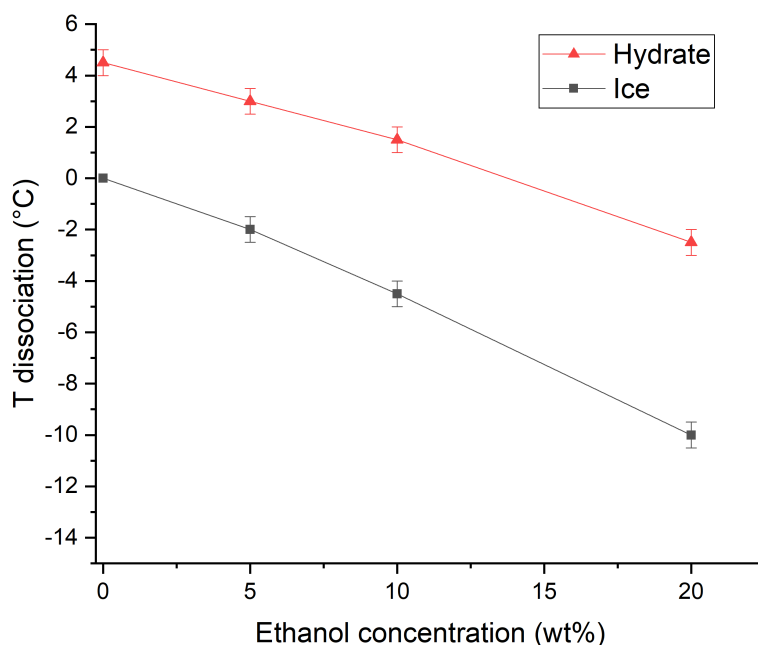


Figure 4.4: Temperature curve as a function of EtOH concentration for ice and THF hydrates dissociation.

The inhibitory effect of ethanol can be clearly observed in the graph as the concentration in each type of sample increases. The most significant effect can be observed when ethanol is added to the samples at a concentration of 20 wt%. In the case of the hydrate curve, it is observed to decrease 7 °C compared to the reference dissociation temperature (4.5 °C). Although methanol has a slightly higher inhibition effect than ethanol or other inhibitors, as seen in Appendix C, ethanol is still an excellent choice when applying a thermodynamic inhibitor. Furthermore, ethanol is a striking option when analyzing its production since this compound can be obtained industrially and through natural means such as starch or sugar in various crops. [24]

4.3 Ethanol production in Ecuador

Ecuador is a multi-diverse country with several sources of production and trade, the most outstanding of which are the oil trade, agriculture, and fishing. Within agriculture, we can also find sugar cane production. This crop is essential to the country since sugarcane is cultivated in almost all provinces. In addition, a great percentage of raw material is used for ethanol distillation (either utilizing the main distilleries in the country, or in an artisanal way). [25] This is due to the large area destined to the sugar cane plantation around Ecuador, approximately 131,000 hectares, from which approximately 6.5 million tons of sugar cane are obtained. Similarly, approximately 525,000 tons of sugar [26, 27, 28] and 130 million liters of ethanol (obtained both for use in gasoline and for industrial or artisanal use) [29] are obtained annually.

Therefore, given Ecuador's remarkable capacity to produce sugar cane and consequently to carry out distillation processes to obtain ethanol, it is interesting to analyze whether this ethanol is feasible for a thermodynamic inhibitor usage.

4.3.1 Ethanol at 96%

The same experiments were carried out for the feasibility analysis of the ethanol obtained by handcrafting as with the other inhibitors tested. The ethanol used in the tests was obtained by processing artisanal ethanol with a purity of 40-50% in a distillation column

at the Universidad Politécnica Nacional (EPN) installations in Quito. Thanks to the collaboration of the EPN in the distillation process, 96% ethanol was finally obtained for the final tests.

Like industrial ethanol, this 96% ethanol belongs to the alcohol family. Each sample was prepared in duplicate for the experimental test, and the average dissociation temperatures obtained are shown in Table 4.1.

Since this ethanol contains only slightly less purity than the previously used industrial

Table 4.1: Dissociation temperatures of ice and THF hydrates as a function of 96% EtOH concentration.

96% EtOH wt%	Water + 96% EtOH T_{dis} (°C)	THF sol.+ 96% EtOH T_{dis} (°C)
0	0	4.5
5	-2	3
10	-4	1.5
20	-9.5	-2

ethanol (96% and 99%, respectively), the dissociation temperature results obtained are very similar to industrial ethanol. To see these results more visually and verify the similarity with the previously obtained ice and hydrate curves, a comparison of both ethanol's ice and hydrate curves can be seen in Figure 4.5.

As can be seen in the graph, both the ice and hydrate curves of both compounds are very similar, with the slight difference of 0.5 °C being the most noticeable in both curves where the ethanol concentration is 20 wt%. Since the points associated with the curves of the industrial ethanol tests are within the margin of error of the points of the 96% ethanol curves, it can be determined that it has an inhibitory effect practically similar to industrial ethanol, so it could be used as a substitute for that compound for hydrate dissociation.

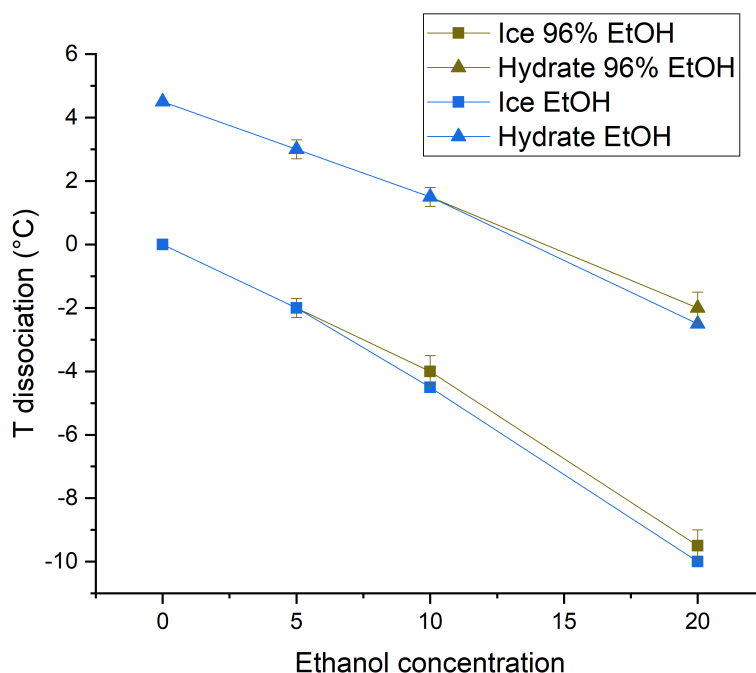


Figure 4.5: Comparison of temperature curves as a function of EtOH (industrial and artisanal) concentration for ice and THF hydrates dissociation.

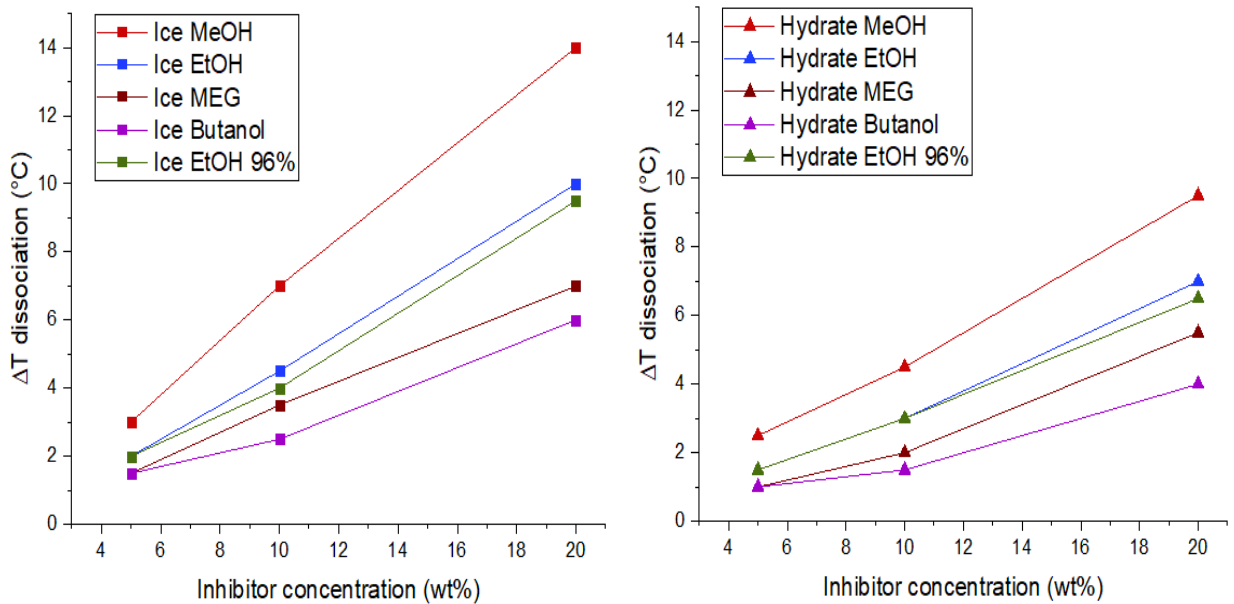
4.4 Analysis and comparison of the inhibitory effects of each additive

Once all the dissociation temperature data were obtained for each test with the different inhibitors, a final analysis of how each compound acts on the inhibitory effect of hydrate formation can be carried out. For this analysis, the dissociation temperatures are not used directly, but the ΔT_{dis} is defined as the difference between a reference dissociation temperature and an experimental dissociation temperature. The reference temperatures are 0 °C for the ice curves and 4.5 °C for the hydrate curves (dissociation temperature of THF hydrates with a THF concentration of 19.2 wt%). The reason for using ΔT for the analysis is to be able to use the Hammerschmidt equation for a thorough and complete analysis of the inhibitory effects present.

Hammerschmidt equation calculates the temperature depression (ΔT) by employing several parameters such as molecular weight, concentration in weight percentage of the inhibitors,

and a constant associated with each one. Since the ΔT of each inhibitor (for both ice and hydrate curves) are already known experimentally, the use of this equation on this occasion is focused on the calculation of each of the K constants associated with the inhibitors to make a comparison of the experimental and theoretical constants. ΔT_{dis} of each inhibitor and all the calculations associated with obtaining the K constants for them can be found in Appendix D; theoretical values of the constants were obtained from Carroll (2020). [1]

Figure 4.6 shows the ΔT curves obtained experimentally for ice and hydrates. In both Figures 4.6a and 4.6b, a similar trend can be observed concerning the effect of the inhibitors, with methanol having the most significant effect and butanol having the least effect. It can also be observed that both ethanols have a very close behavior, with a maximum ΔT difference of 0.5 °C at some points.



(a) Inhibitors concentration vs. ΔT_{dis} for ice curves.

(b) Inhibitors concentration vs. ΔT_{dis} for THF hydrates curves.

Figure 4.6: Thermodynamic inhibitory effects of various inhibitors on the ΔT_{dis} of ice and THF hydrates (19.2 wt%) curves.

The values of K_S (Hammerschmidt constant for water) and K_H (Hammerschmidt constant for inhibitors), both theoretical and experimentally obtained, as well as the absolute error between these values can be found in Tables 4.2 and 4.3. It is important to note from the graphs involving ΔT and the tables of K constants that even having very similar K_S/K_H

values for all inhibitors. All give one effect or another to the dissociation of THF hydrates. This is due to the molecular weight of each compound. Hammerschmidt equation involves the variable M , which pertains to the molecular weight of the inhibitor used. Therefore, the higher the value of M in each case, the lower its inhibitory effect. [30]

Table 4.2: Comparison of theoretical and experimental K_S values.

Inhibitor	K_S Carroll (2020) ¹	K_S Experimental	Absolute Error (%)
Methanol	1861	1826.28	1.87
Ethanol	1861	1842.8	0.98
Butanol	1861	1778.9	4.41
MEG	1861	1768.99	4.94
96% Ethanol	1861	1750.66	5.93

¹ Theoretical value for K_S is always 1861; it's independent of the inhibitor used.

Table 4.3: Comparison of theoretical and experimental K_H values.

Inhibitor	K_H Carroll (2020) ¹	K_H Experimental	Absolute Error (%)
Methanol	1297	1297.62	0.05
Ethanol	1297	1289.96	0.54
Butanol	1297	1185.94	8.56
MEG	1297	1179.33	9.07
96% Ethanol	1297	1243.89	4.09

¹ Carroll establishes that K_H value is always 1297 for all alcohols or glycols.

For each of the K_S and K_H constants associated with the various inhibitors, it can be seen that no absolute error exceeds 10% so that the experimentally obtained values are within the permitted margin of error compared to the theoretical values. However, it is also important to highlight the error of each inhibitor individually. Regarding the K_S values (tests of the effect of the inhibitors on ice dissociation), the theoretical value is 1861, of which 96% ethanol presents the highest error, with a value of 5.93%. This may be associated with the fact that unlike the industrial ethanol used previously (it has the lowest error of all the inhibitors), this ethanol is not completely pure (industrial ethanol is 99% pure). As it was previously obtained in an artisanal way, in addition to not achieving a higher degree of purity in the distillate made afterward, this compound may have contained traces of residues or water that affected its inhibitory effect in the water.

The next most erroneous compounds are butanol and MEG. This trend is also repeated in the K_H values, where the theoretical value is 1297, and these compounds have experimental values with an error of 8.56 and 9.07%, respectively. This could be related to these compounds having higher molecular weights, so their effectiveness decreases. So, considering both K , in general analysis, methanol and ethanol would be the best inhibitors to use for hydrate inhibition because of their excellent performance. The following best would be the 96% artisanal ethanol variant, which, having a moderately high error, might not be considered suitable. However, as the error values are within the 10% allowed, it could also be used, sacrificing slight differences in dissociation temperature for the possible economic convenience of its acquisition.

After the effectiveness analysis of the inhibitors, in order to obtain a more complete analysis, the economic desirability between compounds can be taken into account, and a final decision can be made considering all possible factors.

4.5 Economic study: greater convenience among inhibitors.

Between alcohols and glycols, it is known that compounds within the alcohol family are always more economically convenient. However, although glycols are worth up to two times as much as some alcohol, these compounds are not as volatile and can be regenerated to lower costs. It is also necessary to consider the losses and the uniform distribution in the raw material flow, where MEG presents more problems at both points. Therefore, it is necessary to use more of this compound; alcohols such as methanol do not present many inconveniences with these factors. [31]

In order to carry out a study of the economic suitability of the industrial compounds used, (except for butanol, since it has not proven to be very effective and there are already other options within the alcohol family) the global prices (current values in 2023) of each one of them are as follows:

- **Methanol:** according to the Methanex Corporation website, the cost of methanol

for industrial use at global level is approximately 1 USD/L.[32]

- **Ethanol:** according to the GlobalPetrolPrices website, the cost of ethanol for industrial use at global level is 1.30 USD/L. [33]
- **MEG:** according to the Acuro Organics Limited website, the cost of monoethylene glycol for industrial use at global level is 1.46 USD/L (conversion from Rs to USD). [34]

4.5.1 Artisanal 96% ethanol: cost on the Ecuadorian market

In 2019, Petroecuador signed a purchase agreement for 110.5 million liters of ethanol per liter of artisanal ethanol nationwide, where the purchase price would be USD 0.83 per liter. [35] Finally, the price established in the pilot plan was a purchase price of 0.84 USD/L of ethanol. At present (2023), the same purchase price is still maintained for artisanal ethanol. [36]

Chapter 5

Conclusions

- As THF hydrates form a crystalline arrangement with cavities very similar to hydrates formed by hydrocarbons, they were very convenient to study their behavior at the time of their formation and dissociation without the need to use a highly pressurized setup, making it possible to carry out a good control of each experimental set.
- All the chosen thermodynamic inhibitor type compounds belong to the group of alcohols or glycols; these types of compounds are usually used as hydrate inhibitors due to the presence of -OH groups in their composition, which are responsible for their effect by interacting with the hydrogen bonds of the water in the hydrates to weaken them. However, butanol is not normally used as an inhibitor, so the tests carried out with it served to identify whether it could also be used as a potential hydrate inhibitor.
- Of the proposed industrial inhibitors (methanol, ethanol, butanol and MEG), individual tests were carried out with respect to the dissociation temperature of ice and THF hydrates, in order to know their performance. Based on the collected data of dissociation temperature based on the used concentration of each inhibitor, plots involving ΔT were prepared. From these graphs, it can be generally established that the compound with the best inhibitory effect is methanol, and the one with the least effect is butanol.
- Using the Hammerschmidt equation, based on the ΔT obtained experimentally, the

Hammerschmidt constants for water (K_S) and the different inhibitors (K_H) were found. To conclude the final analysis based on the K s obtained, the absolute error between the theoretical and experimental values was used to decide, confirming that in general methanol and ethanol (industrial and artisanal) are the best inhibitors to use, in terms of effectiveness.

- As the second best inhibitor is ethanol, of which an alternative compound is also presented, being 96% ethanol obtained in an artisanal way. The performance of this compound is very similar to that of industrial ethanol, being that only in certain concentrations it differs 0.5 °C from the dissociation temperature of the industrial compound.
- Through an economic analysis of the global market, also taking into account factors such as losses, recoveries and uniform distribution in the raw material, it was determined that the most economically convenient options also coincide in methanol and ethanol.
- Since 96% artisanal methanol is a variant of industrial ethanol, it was also taken into account for an economic study. Considering Ecuador's agricultural potential with respect to sugarcane plantation, which is a means of obtaining artisanal ethanol, in addition to the already existing high domestic production and sales market for artisanal ethanol, its domestic market was analyzed. Handmade ethanol is marketed at a value of 0.84 USD/L, which is a very economical value. If the possibility of using this ethanol as an inhibitor is analyzed, it could be convenient for the hydrocarbon industries, since the difference in its effectiveness with that of industrial ethanol is minimal, while the difference in its prices in the market is more notorious, with artisanal ethanol being the most convenient in the economic aspect.

Bibliography

- [1] J. Carroll, *Natural gas hydrates: a guide for engineers*, 2nd ed. Gulf Professional Publishing, 2020.
- [2] Y. F. Makogon, “Natural gas hydrates—a promising source of energy,” *Journal of natural gas science and engineering*, vol. 2, no. 1, pp. 49–59, 2010.
- [3] C. Koh, R. E. Westacott, W. Zhang, K. Hirachand, J. Creek, and A. Soper, “Mechanisms of gas hydrate formation and inhibition,” *Fluid Phase Equilibria*, vol. 194, pp. 143–151, 2002.
- [4] E. D. Sloan Jr and C. A. Koh, *Clathrate hydrates of natural gases*. CRC press, 2008.
- [5] E. D. Sloan, *Natural gas hydrates in flow assurance*. Gulf Professional Publishing, 2010.
- [6] IEA, “Gas market report, q1 2022 – analysis,” Jan 2022. [Online]. Available: <https://www.iea.org/reports/gas-market-report-q1-2022>
- [7] Enerdata, “Natural gas production,” Jan 2022. [Online]. Available: <https://yearbook.enerdata.net/natural-gas/world-natural-gas-production-statistics.html>
- [8] PrimiciasEc, “El mercado de gas natural suma nuevos actores con greenpower y gasvesubio,” Jan 2022. [Online]. Available: <https://www.primicias.ec/noticias/economia/gas-natural-competidores-greenpower-gasvesubio/>
- [9] J. G. Speight, *Natural gas: a basic handbook*. Gulf Professional Publishing, 2018.
- [10] M. Ricaurte, J. M. Fernández, and A. Vilorio, “An improved method for calculating critical temperatures and critical pressures in natural gas mixtures with up to nc11

- hydrocarbons,” *Oil & Gas Science and Technology–Revue d’IFP Energies nouvelles*, vol. 74, p. 53, 2019.
- [11] F. A. Carey, “Hydrocarbon,” Sep 2022. [Online]. Available: <https://www.britannica.com/science/hydrocarbon>
- [12] L. Rovetto and C. Peters, “Storage of hydrogen as gas hydrates and its near-future impact on the oil, gas, chemical and automotive industry,” 2016.
- [13] G. A. Jeffrey, “Hydrate inclusion compounds,” *Journal of inclusion phenomena*, vol. 1, no. 3, pp. 211–222, 1984.
- [14] H. Müller, “Tetrahydrofuran,” *Ullmann’s Encyclopedia of Industrial Chemistry*, 2000.
- [15] P. Wilson, D. Lester, and A. Haymet, “Heterogeneous nucleation of clathrates from supercooled tetrahydrofuran (thf)/water mixtures, and the effect of an added catalyst,” *Chemical engineering science*, vol. 60, no. 11, pp. 2937–2941, 2005.
- [16] T. M. Vlastic, P. D. Servio, and A. D. Rey, “Thf hydrates as model systems for natural gas hydrates: comparing their mechanical and vibrational properties,” *Industrial & Engineering Chemistry Research*, vol. 58, no. 36, pp. 16 588–16 596, 2019.
- [17] M. Stewart, *Surface Production Operations: Vol 2: Design of Gas-Handling Systems and Facilities*. Gulf Professional Publishing, 2014, vol. 2.
- [18] R. Chebbi, M. Qasim, and N. A. Jabbar, “Optimization of triethylene glycol dehydration of natural gas,” *Energy Reports*, vol. 5, pp. 723–732, 2019.
- [19] H. A. Farag, M. M. Ezzat, H. Amer, and A. W. Nashed, “Natural gas dehydration by desiccant materials,” *Alexandria Engineering Journal*, vol. 50, no. 4, pp. 431–439, 2011.
- [20] J. Pomicpic, R. Ghosh, and M. A. Kelland, “Non-amide polymers as kinetic hydrate inhibitors maleic acid/alkyl acrylate copolymers and the effect of ph on performance,” *ACS omega*, vol. 7, no. 1, pp. 1404–1411, 2021.

- [21] H. Williams, T. Herrmann, M. Jordan, and C. McCallum, “The impact of thermodynamic hydrate inhibitors (meg and methanol) on scale dissolver performance,” in *SPE International Oilfield Scale Conference and Exhibition*. OnePetro, 2016.
- [22] O. T. Olabisi, I. S. Sunday, and D. Appah, “Lpg hydrate formation and prevention using ethanol and methanol,” in *SPE Nigeria Annual International Conference and Exhibition*. OnePetro, 2015.
- [23] N. P. Cheremisinoff, *Industrial solvents handbook, revised and expanded*. CRC press, 2003.
- [24] F. Santos, P. Eichler, J. H. de Queiroz, and F. Gomes, “Production of second-generation ethanol from sugarcane,” in *Sugarcane biorefinery, technology and perspectives*. Elsevier, 2020, pp. 195–228.
- [25] M. Ricaurte, S. Luna, S. Mosquera, J. Sarmas, J. Zenteno, and A. Vilorio, “Diseño de una planta para la producción de etanol a partir de la caña de azúcar: aplicación en la zona norte de ecuador,” in *Bionatura Conference Series*, vol. 2, no. 1, 2019, pp. 1–7.
- [26] A. M. Sánchez, T. Vayas, F. Mayorga, and C. Freire, 2020. [Online]. Available: https://fca.uta.edu.ec/v4.0/images/OBSERVATORIO/dipticos/Diptico_N39.pdf
- [27] “Luego de siete años aumenta el precio de la tonelada de caña de azúcar,” Jun 2022. [Online]. Available: <https://www.agricultura.gob.ec/luego-de-siete-anos-aumenta-el-precio-de-la-tonelada-de-cana-de-azucar/>
- [28] A. M. Sánchez, T. Vayas, F. Mayorga, and C. Freire, 2020. [Online]. Available: https://fca.uta.edu.ec/v4.0/images/OBSERVATORIO/dipticos/Diptico_N39.pdf
- [29] P. T. Franco, “Ingenios iniciaron la zafra y se prevé producción de 10,3 millones de sacos de azúcar de 50 kilos,” Jun 2021. [Online]. Available: <https://www.eluniverso.com/noticias/economia/ingenios-iniciaron-la-zafra-y-se-preve-produccion-de-103-millones-de-sacos-de-azucar-de-50-kilos>

- [30] J. M. Campbell, R. N. Maddox, L. L. Lilly, and R. A. Hubbard, *Gas conditioning and processing*. Campbell Petroleum Series Norman, Oklahoma, 1984, vol. 1.
- [31] K. Snow-McGregor and M. Moshfeghian, “Thermodynamic hydrate inhibitors – how do they compare?” Nov 2020. [Online]. Available: <https://www.jmcampbell.com/tip-of-the-month/2020/11/thermodynamic-hydrate-inhibitors-how-do-they-compare/>
- [32] M. Corporation, “Methanex. the power of agility.” [Online]. Available: <https://www.methanex.com/>
- [33] GlobalPetrolPrices, “Ethanol prices, litre, 19-jun-2023.” [Online]. Available: https://www.globalpetrolprices.com/ethanol_prices/
- [34] A. O. Limited, “Acuro organic limited. glycols.” [Online]. Available: <https://www.chemicals99.com/glycols.html>
- [35] M. Pacheco, “La compra de etanol local para producir la ecopaís se retoma,” Feb 2019. [Online]. Available: <https://www.elcomercio.com/actualidad/negocios/etanol-ecopais-ministerio-energia-biocombustible.html>
- [36] M. Orozco, “Usd 78 millones costaría vender gasolina eco plus en todo el país,” Aug 2022. [Online]. Available: <https://www.primicias.ec/noticias/economia/eco-plus-nueva-gasolina-ecuador/>
- [37] X. Lv, D. Lu, Y. Liu, S. Zhou, J. Zuo, H. Jin, B. Shi, and E. Li, “Study on methane hydrate formation in gas–water systems with a new compound promoter,” *RSC advances*, vol. 9, no. 57, pp. 33 506–33 518, 2019.
- [38] W. Ke, T. M. Svartaas, and D. Chen, “A review of gas hydrate nucleation theories and growth models,” *Journal of Natural Gas Science and Engineering*, vol. 61, pp. 169–196, 2019.
- [39] K. You, P. B. Flemings, A. Malinverno, T. Collett, and K. Darnell, “Mechanisms of methane hydrate formation in geological systems,” *Reviews of Geophysics*, vol. 57, no. 4, pp. 1146–1196, 2019.

Appendices

Appendix A

Natural gas production in 2021

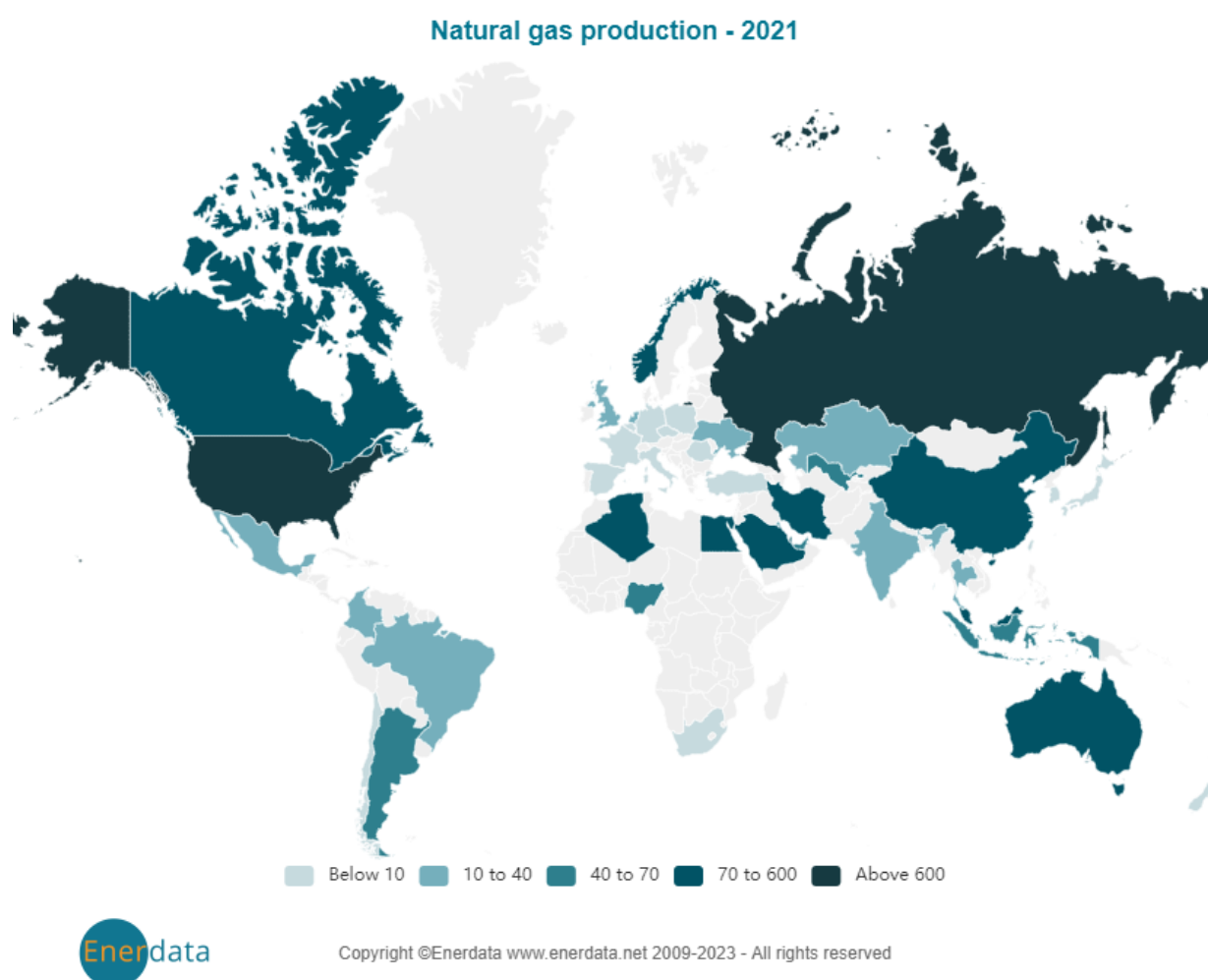


Figure A.1: Natural gas production in 2021 (units in bcm).

Appendix B

Hydrates formation and dissociation processes

Some questions that arise in the hydrate field are about how they come to be formed, what factors influence their formation, how much time is necessary to fully develop the hydrates, or even how long or what is necessary for their dissociation. The formation of hydrates is due to the phenomena of nucleation and hydrate growth. [4]

As shown in Figure B.1, in this process, water complexes and guest molecules in an unstable state start to grow little by little and then start to disperse until they reach the critical point of their size in a stable situation. [37] This occurs at microscopic levels and is a stochastic process (in other words, it evolves depending on other variables), so it is somewhat complicated to study. However, nucleation is practically the beginning and the key to studying hydrate formation.

For this reason, two types of techniques involving hydrate formation are generally used in this study: analysis of hydrate formation based on gas consumption over time, and hydrate formation and dissociation based on varying pressure and temperature conditions. [38]

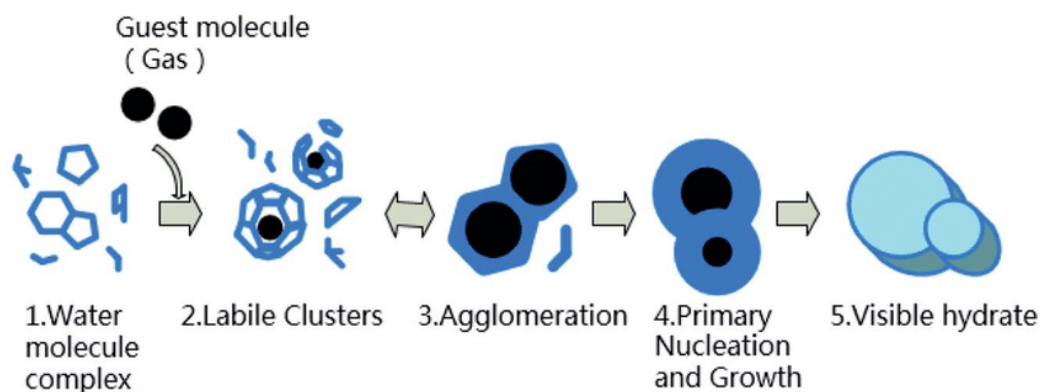


Figure B.1: Hydrate nucleation process scheme. (Lv, Xiaofang et al., 2019)

B.1 Hydrate formation over time

For this experiment, the gas consumption that occupies the hydrate formation over time is studied, presented in a diagram in Figure B.2. It can be carried out in an agitation system, maintaining constant operating conditions of pressure and temperature, where the gas will be supplied from a reservoir. As can be seen in the diagram, there are four differentiated stages, which correspond to the nucleation and growth processes of the hydrates.

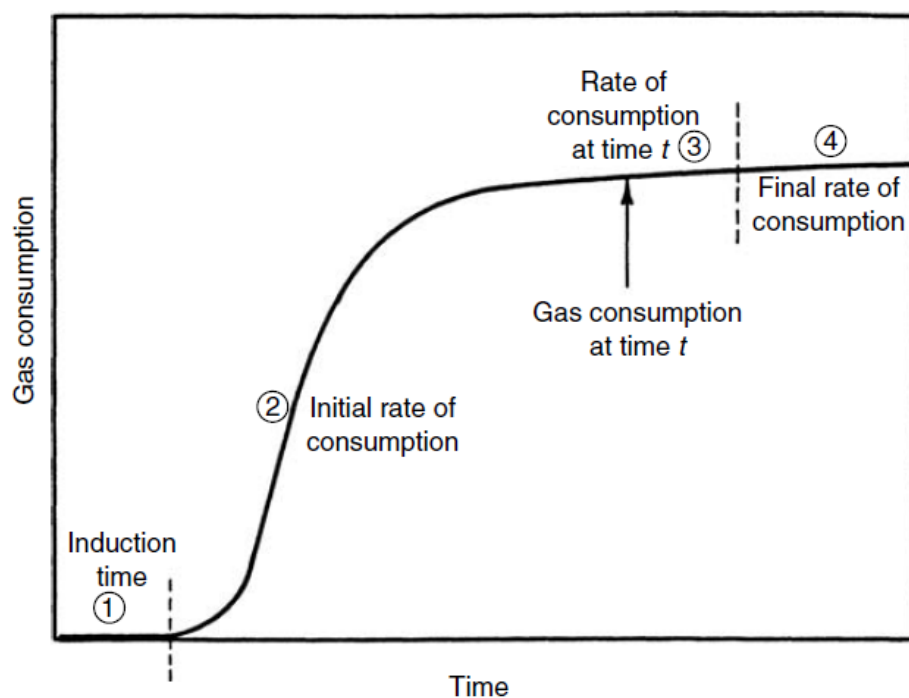


Figure B.2: Gas consumption vs. time diagram for hydrate formation. (Sloan and Koh, 2008)

1. **Induction time:** at this stage, the time it takes for the crystal nuclei to form is established. Here it is said that the nucleation process begins since a volume of the hydrate phase appears considerable enough to be detected. At this stage, the pressure and temperature conditions are already optimal for hydrate formation; however, hydrates are not fully formed due to their metastability (a period in which the non-equilibrium state remains long).
2. **Initial rate of consumption:** at this stage, hydrate growth begins as gas guest molecules enter the cages of the crystalline structure.
3. **Rate of consumption at time t :** at this stage, the curve slope decreases with time, and this is because, at the same time that gas is consumed, water is also consumed in the formation of hydrates.
4. **Final rate of consumption:** the slope of the curve at this point decreases with time, and this is because at the same time that gas is consumed, water is also consumed in the formation of hydrates. [4, 38]

B.2 Hydrate formation and dissociation varying P and T

For P-T experiments, another type of hydrate formation and dissociation mechanism is studied based on the temperature and pressure conditions variation. It can be carried out in an agitation system, maintaining a constant volume (fixed amount of water and gas). To proceed with the analysis, we will take as an example B.3, which shows the methane hydrate formation diagram and its different stages.

- **A-B:** the period between points A and B takes a few hours and corresponds to the induction time, where the temperature (and consequently the pressure) gradually begins to decrease, and the hydrate formation begins at point B. During this time and according to the curve presented, it is observed that it passes through point D, corresponding to the hydrate equilibrium in both pressure and temperature. However, despite having the optimum conditions for an immediate hydrate formation, that does not occur. This is due to the initial metastability of the system.

- **B-C:** a large pressure drop can be seen from points B to C. This is because significant hydrate growth is taking place, and when point C is finally reached, it stops because the critical moment of formation has been reached.
- **C-D:** from points C to D, dissociation of the hydrates takes place because the temperature and pressure start to increase. When point D is reached, the hydrates are already completely dissociated since they have reached the equilibrium condition based on temperature and pressure (in this phase, there is no longer the metastability present at the beginning). [4, 39]

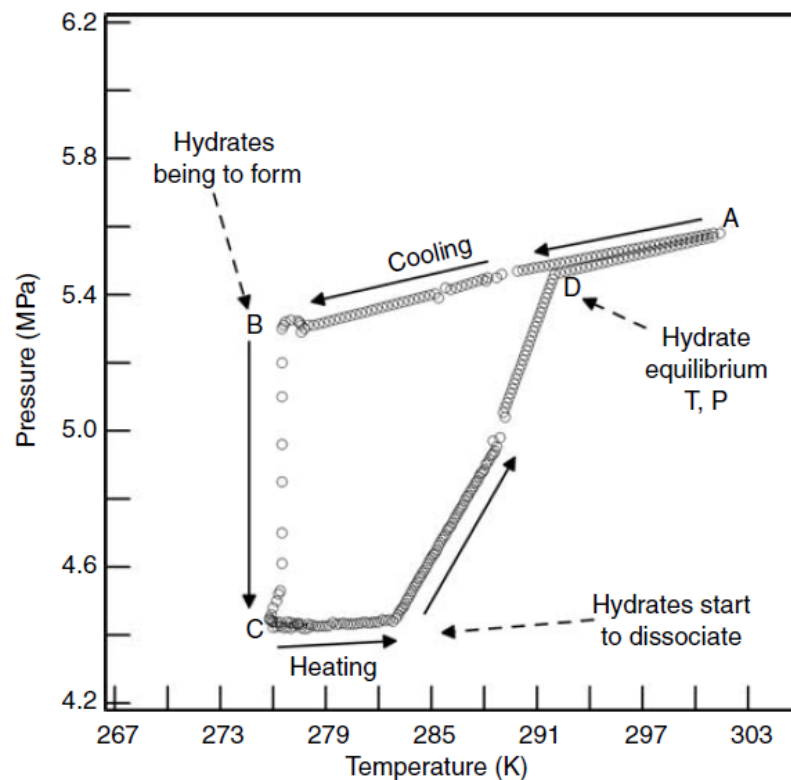


Figure B.3: Pressure vs. temperature diagram for methane hydrate formation. (Sloan and Koh, 2008)

Appendix C

Thermodynamic effects on THF hydrates dissociation of various inhibitors

C.1 Methanol

Table C.1: Dissociation temperatures of ice and THF hydrates as a function of MeOH concentration.

Methanol wt%	Water + MeOH T_{dis} (°C)	THF sol. + MeOH T_{dis} (°C)
0	0	4.5
5	-3	2
10	-7	0
20	-14	-5

C.2 Butanol

Table C.2: Dissociation temperatures of ice and THF hydrates as a function of butanol concentration.

Butanol wt%	Water + Butanol T_{dis} (°C)	THF sol. + Butanol T_{dis} (°C)
0	0	4.5
5	-1.5	3.5
10	-2.5	3
20	-6	0.5

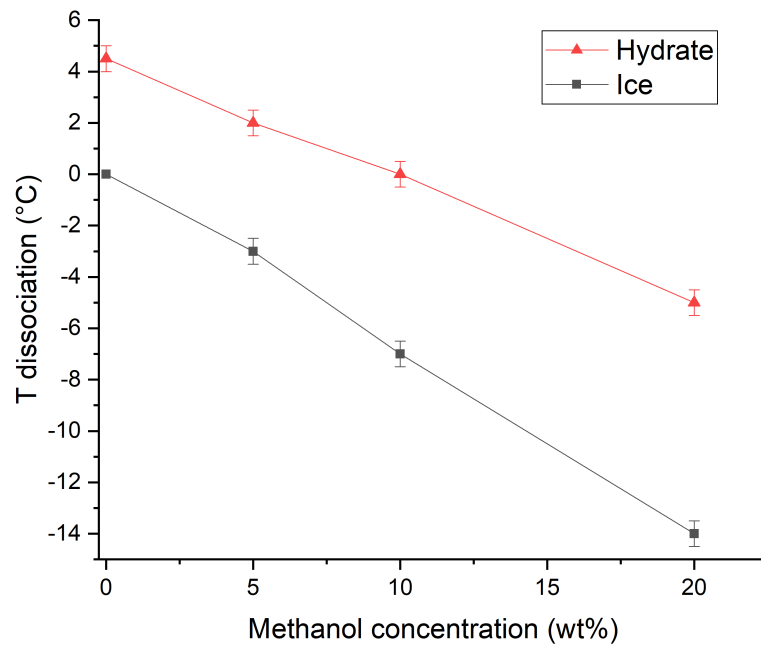


Figure C.1: Temperature curve as a function of MeOH concentration for ice and THF hydrates dissociation.

C.3 Monoethylene Glycol (MEG)

Table C.3: Dissociation temperatures of ice and THF hydrates as a function of MEG concentration.

MEG wt%	Water + MEG T_{dis} (°C)	THF sol. + MEG T_{dis} (°C)
0	0	4.5
5	-1.5	3.5
10	-3.5	2.5
20	-7	-1

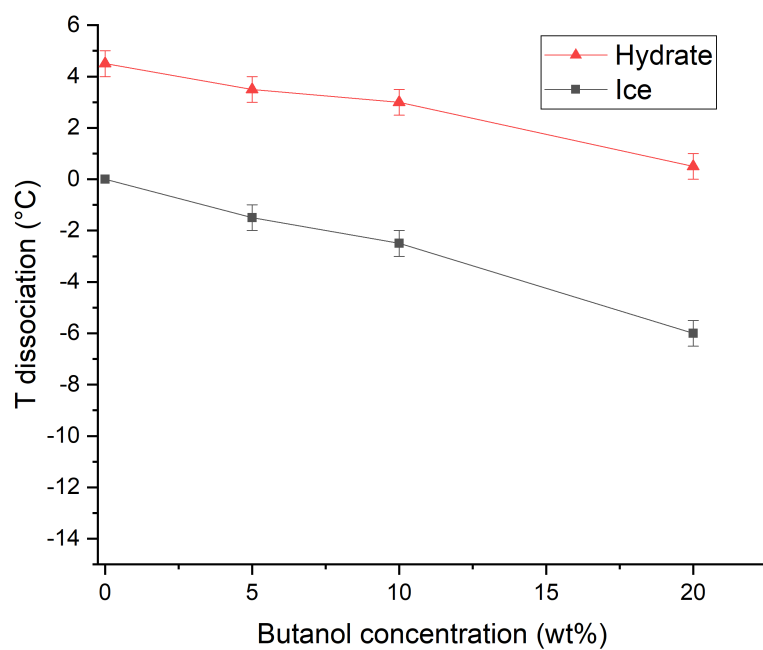


Figure C.2: Temperature curve as a function of butanol concentration for ice and THF hydrates dissociation.

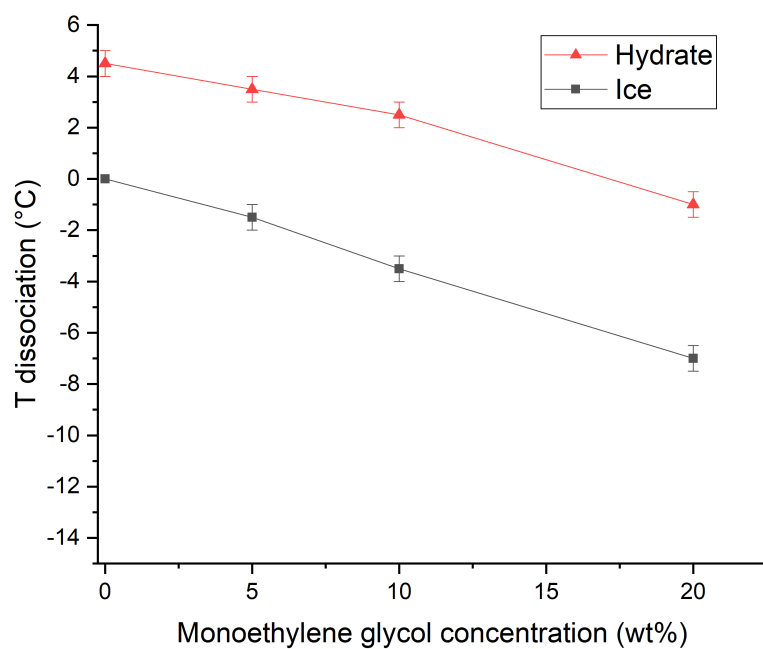


Figure C.3: Temperature curve as a function of MEG concentration for ice and THF hydrates dissociation.

Appendix D

Hammerschmidt's equation: calculation of K constants associated with each inhibitor

To find the K_H for each compound, both for the ice and hydrate curves, the following equation is used

$$\Delta T = \frac{K_H}{M} \left(\frac{W}{100 - W} \right)$$

Microsoft Excel was used for K calculations, being each constant obtained as follows:

1. ΔT is defined as the difference of the reference dissociation temperature (in the case of ice, 0 °C; in the case of hydrates, 4.5 °C) and the experimental dissociation temperature (in dependence on the concentration of the inhibitor used).
2. The molecular weight of each inhibitor (M), as well as its concentration in weight percentage used (W) and $(100-W)/W$ are defined to facilitate the calculations.
3. A random value of K is chosen to find ΔT_{calc} , which is obtained by multiplying K by $(100-W)/W$ (for each inhibitor concentration value) and dividing the result by M. This is done to find the absolute error between the experimental ΔT and ΔT_{calc} values.
4. Once the absolute errors have been obtained depending on the concentration, they are averaged. With the help of the "Solver" tool integrated in Excel, an adjustment

of the K value is made by minimizing the average error, obtaining the final K value associated with the inhibitor used.

This process is performed with both ice and hydrate tests. Although K_H is used in the Hammerschmidt equation to represent the Hammerschmidt constant, the nomenclature K_S and K_H is used to represent the K constants of each inhibitor associated with the ice and hydrate tests, respectively.

D.1 Methanol

Based on the data reflected in Table D.1, the values of the methanol-associated constants for ice and hydrates found in Figure D.1 are $K_S=1826.28$ and $K_H=1297.62$.

Table D.1: ΔT_{dis} of ice and THF hydrates as a function of methanol concentration.

Methanol wt%	Ice ΔT_{dis} (°C)	Hydrate ΔT_{dis} (°C)
5	3	2.5
10	7	4.5
20	14	9.5

	A	B	C	D	E	F	G	H
10								
11		Ice	0 °C					
12		Methanol	32,04 g/mol (M)			Ks	1826,28	
13								
14		Delta T	W	(100-W)/W		Delta T calc	Error	
15		0	0	0		0		
16		3	5	0,052631579		2,999999999	2,9874E-07	
17		7	10	0,111111111		6,333333331	9,52380979	
18		14	20	0,25		14,25	1,78571398	
19							3,76984136	
20								
21								
22		Hydrate	4,5 °C					
23		Methanol	32,04 g/mol (M)			Kh	1297,62	
24								
25		Delta T	W	(100-W)/W		Delta T calc	Error	
26		0	0	0		0		
27		2,5	5	0,052631579		2,13157895	14,7368422	
28		4,5	10	0,111111111		4,5	7,912E-08	
29		9,5	20	0,25		10,125	6,57894728	
30							7,10526318	
31								

Figure D.1: Excel spreadsheet for the estimation of K_S and K_H associated with methanol.

D.2 Ethanol

Based on the data reflected in Table D.2, the values of the methanol-associated constants for ice and hydrates found in Figure D.2 are $K_S=1842.8$ and $K_H=1289.96$.

Table D.2: ΔT_{dis} of ice and THF hydrates as a function of ethanol concentration.

Ethanol wt%	Ice ΔT_{dis} (°C)	Hydrate ΔT_{dis} (°C)
5	2	1.5
10	4.5	3
20	10	7

	A	B	C	D	E	F	G	H
10								
11		Ice	0 °C					
12		Ethanol	46,07 g/mol (M)			Ks	1842,80	
13								
14		Delta T	W	(100-W)/W		Delta T calc	Error	
15		0	0	0		0		
16		2	5	0,052631579		2,105262401	5,26312007	
17		4,5	10	0,111111111		4,444442848	1,23460339	
18		10	20	0,25		9,999996407	3,5931E-05	
19							2,1659198	
20								
21								
22		Hydrate	4,5 °C					
23		Ethanol	46,07 g/mol (M)			Kh	1289,96	
24								
25		Delta T	W	(100-W)/W		Delta T calc	Error	
26		0	0	0		0		
27		1,5	5	0,052631579		1,473684029	1,75439804	
28		3	10	0,111111111		3,111110729	3,70369095	
29		7	20	0,25		6,999999139	1,2294E-05	
30							1,8193671	
31								

Figure D.2: Excel spreadsheet for the estimation of K_S and K_H associated with ethanol.

D.3 Butanol

Based on the data reflected in Table D.3, the values of the methanol-associated constants for ice and hydrates found in Figure D.3 are $K_S=1778.9$ and $K_H=1185.94$.

Table D.3: ΔT_{dis} of ice and THF hydrates as a function of butanol concentration.

Butanol wt%	Ice ΔT_{dis} (°C)	Hydrate ΔT_{dis} (°C)
5	1.5	1
10	2.5	1.5
20	6	4

	A	B	C	D	E	F	G	H
10								
11		Ice		0 °C				
12		Butanol		74,121 g/mol (M)		Ks	1778,90	
13								
14		Delta T	W	(100-W)/W		Delta T calc	Error	
15		0	0	0		0		
16		1,5	5	0,052631579		1,263157607	15,7894928	
17		2,5	10	0,111111111		2,66666606	6,6666424	
18		6	20	0,25		5,999998635	2,2752E-05	
19							7,485386	
20								
21								
22		Hydrate		4,5 °C				
23		Butanol		74,121 g/mol (M)		Kh	1185,94	
24								
25		Delta T	W	(100-W)/W		Delta T calc	Error	
26		0	0	0		0		
27		1	5	0,052631579		0,842105139	15,7894861	
28		1,5	10	0,111111111		1,777777516	18,5185011	
29		4	20	0,25		3,999999412	1,4697E-05	
30							11,4360006	
31								

Figure D.3: Excel spreadsheet for the estimation of K_S and K_H associated with butanol.

D.4 Monoethylene glycol

Based on the data reflected in Table D.4, the values of the methanol-associated constants for ice and hydrates found in Figure D.4 are $K_S=1768.99$ and $K_H=1179.33$.

Table D.4: ΔT_{dis} of ice and THF hydrates as a function of MEG concentration.

MEG wt%	Ice ΔT_{dis} (°C)	Hydrate ΔT_{dis} (°C)
5	1.5	1
10	3.5	2
20	7	5.5

D.5 96% Ethanol

Based on the data reflected in Table D.5, the values of the methanol-associated constants for ice and hydrates found in Figure D.5 are $K_S=1750.66$ and $K_H=1243.89$.

Table D.5: ΔT_{dis} of ice and THF hydrates as a function of 96% ethanol concentration.

96% Ethanol wt%	Ice ΔT_{dis} (°C)	Hydrate ΔT_{dis} (°C)
5	2	1.5
10	4	3
20	9.5	6.5

	A	B	C	D	E	F	G	H
10								
11		Ice	0 °C					
12		MEG	62,07 g/mol (M)			Ks	1768,99	
13								
14		Delta T	W	(100-W)/W		Delta T calc	Error	
15		0	0	0		0		
16		1,5	5	0,052631579		1,499999235	5,0995E-05	
17		3,5	10	0,111111111		3,166665052	9,52385566	
18		7	20	0,25		7,124996367	1,78566238	
19							3,76985635	
20								
21								
22		Hydrate	4,5 °C					
23		MEG	62,07 g/mol (M)			Kh	1179,33	
24								
25		Delta T	W	(100-W)/W		Delta T calc	Error	
26		0	0	0		0		
27		1	5	0,052631579		0,999999698	3,02E-05	
28		2	10	0,111111111		2,111110474	5,5552368	
29		5,5	20	0,25		4,749998566	13,6363897	
30							6,39731453	
31								

Figure D.4: Excel spreadsheet for the estimation of K_S and K_H associated with MEG.

	A	B	C	D	E	F	G	H
10								
11		Ice	0 °C					
12		96% Ethanol	46,07 g/mol (M)			Ks	1750,66	
13								
14		Delta T	W	(100-W)/W		Delta T calc	Error	
15		0	0	0		0		
16		2	5	0,052631579		1,999999116	4,4198E-05	
17		4	10	0,111111111		4,222220356	5,5555089	
18		9,5	20	0,25		9,499995801	4,4198E-05	
19							1,85186577	
20								
21								
22		Hydrate	4,5 °C					
23		96% Ethanol	46,07 g/mol (M)			Kh	1243,89	
24								
25		Delta T	W	(100-W)/W		Delta T calc	Error	
26		0	0	0		0		
27		1,5	5	0,052631579		1,42105263	5,263158	
28		3	10	0,111111111		2,999999997	1,1361E-07	
29		6,5	20	0,25		6,749999992	3,84615373	
30							3,03643728	
31								

Figure D.5: Excel spreadsheet for the estimation of K_S and K_H associated with 96% ethanol.